Lithos 162–163 (2013) 70–87

Contents lists available at SciVerse ScienceDirect

Lithos

journal homepage: www.elsevier.com/locate/lithos

Zircon U–Pb age constraints from Iran on the magmatic evolution related to Neotethyan subduction and Zagros orogeny

Han-Yi Chiu [a], Sun-Lin Chung [a,*], Mohammad Hossein Zarrinkoub [b], Seyyed Saeid Mohammadi [b], Mohammad Mahdi Khatib [b], Yoshiyuki Iizuka [c]

[a] Department of Geosciences, National Taiwan University, Taipei, Taiwan
[b] Department of Geology, Birjand University, Birjand, Iran
[c] Institute of Earth Sciences, Academia Sinica, Taipei, Taiwan

ARTICLE INFO

Article history:
Received 12 July 2012
Accepted 11 January 2013
Available online 20 January 2013

Keywords:
Zircon U–Pb age
UDMA
SSZ
Iran
Neotethyan subduction
Zagros orogeny

ABSTRACT

This study reports zircon LA-ICPMS U–Pb ages of 50 igneous rock samples from the Urumieh–Dokhtar magmatic arc (UDMA) and Sanandaj–Sirjan structural zone (SSZ) in Iran. These results, together with literatures and our unpublished age data, better delineate the magmatic evolution related to the Neotethyan subduction and subsequent Zagros orogeny that resulted from the Arabia–Eurasia collision. Subduction-related magmatism was active during Jurassic time, as evidenced by the presence of widespread I-type granitoids from the Middle to Late Jurassic (176–144 Ma) in the SSZ. After a protracted magmatic quiescence in the Early Cretaceous, igneous activity renewed inland in the UDMA from which we identify Late Cretaceous granitoids (81–72 Ma) in Jiroft and Bazman areas, the southeastern segment of the UDMA. The UDMA volcanism was most active and widespread during the Eocene and Oligocene (55–25 Ma), much longer lasting than previously thought as just an Eocene pulse. Such a prolonged igneous "flare-up" event in the UDMA can be correlated to Armenia where coeval calc-alkaline rocks are common. The UDMA magmatism ceased progressively from northwest to southeast, with magmatic activities ending the Early Miocene (ca. 22 Ma) in Meghri, the Middle Miocene (ca. 16 Ma) in Kashan and the Late Miocene (ca. 10–6 Ma) in Anar, respectively. The southeastward magmatic cessation is consistent with the notion of oblique and diachronous collision between Arabia and Eurasia. Post-collisional volcanism started ca. 11 Ma in Saray, east off the Urumieh Lake, which, along with later eruptions in Sahand (6.5–4.2 Ma) and Sabalan (≤0.4 Ma) volcanoes, forms a compositionally unique component of the vast volcanic field covering much of the Lesser Caucasus, NW Iran and eastern Anatolia regions.

1. Introduction

The Zagros orogen of Iran, as a member of the Alpine–Himalayan orogenic belt, consists of several NW–SE trending parallel subdivisions such as the Urumieh–Dokhtar magmatic arc (UDMA), the Sanandaj–Sirjan structural zone (SSZ) and the Zagros fault-and-thrust belt (or Zagros Main Range). Its formation has been attributed to the long-standing convergence and interaction between Eurasia/Laurasia and Gondwana-derived terranes (Alavi, 1994; Berberian and King, 1981; Ghasemi and Talbot, 2006; Mohajjel et al., 2003). Despite a wealth of recent investigations, the Zagros orogen remains much less documented than its adjacent counterparts, e.g., the Himalayas, the Alps or Anatolia of Turkey. Similar to other segments of the Alpine–Himalayan belt, the Zagros orogeny formed as a consequence of closure of the Neo-Tethys Ocean. The timing of this closure, concerning when Arabia started colliding with Eurasia, however, has been highly controversial, ranging from the Late Cretaceous to as late as the Pliocene (cf. Agard et al., 2011; for review). The position of the suture zone itself, regarded by most workers as the Bitlis–Zagros Suture that lies along the Main Zagros Thrust (Fig. 1), is also still discussed (Alavi, 1994; Moghadam et al., 2010). In general, the Neotethyan subduction is widely considered as the key process that had operated from the Jurassic to Tertiary to form the arc magmatism not only in the UDMA (e.g., Alavi, 1994; Berberian and King, 1981; Omrani et al., 2008; Verdel et al., 2011), but also in the SSZ (e.g., Aghazadeh et al., 2010; Arvin et al., 2007; Baharifar et al., 2004; Ghasemi and Talbot, 2006; Mohajjel et al., 2003). Although an increasing amount of geochronological results have been published in the last decade for various rocks from Iran (Fig. 1 and Table A1), good quality age data from the UDMA that are urgently needed for constraining the Neotethyan arc evolution and Zagros orogeny remain very limited.

In this paper, we report the age results obtained by a detailed geochronological study of the UDMA. These include zircon LA-ICPMS U–Pb

* Corresponding author. Tel.: +886 8369 1242 (voice); fax: +886 2363 6095.
E-mail address: sunlin@ntu.edu.tw (S.-L. Chung).

0024-4937/$ – see front matter
http://dx.doi.org/10.1016/j.lithos.2013.01.006

ages of 46 samples and whole-rock Ar–Ar ages of 12 samples from the UDMA, together with zircon U–Pb ages of four granitoids from adjacent areas in the SSZ (Fig. 1). Our new age results are combined with (1) literature age data from the UDMA and SSZ, and (2) published and our unpublished age data of related igneous rocks from Armenia, Georgia, Anatolia and elsewhere Iran, and thus significantly improve our understanding of the Neotethyan magmatic evolution in Iran and neighboring regions. This study, moreover, provides important age constraints that signify the timing and fashion of the Arabia–Eurasia collision and its post-collisional volcanism.

2. Background and previous studies

The UDMA (Fig. 1) represents a subduction-related, linear magmatic belt that consists of voluminous volcanic successions, with minor intrusive rocks, along the active margin of the southern Iranian plate. Being a major component across the entire Zagros orogen (Alavi, 1994, 2004), it has long been interpreted as an Andean-type magmatic arc produced by the subduction of the Neotethyan oceanic lithosphere beneath the Iranian plate (Alavi, 1980, 1994; Berberian and Berberian, 1981; Berberian et al., 1982). The volcanic successions, up to ~4 km thick in localities, are composed largely of calc-alkaline rocks occurring as lava flows, pyroclastic layers, tuffs and ignimbrites (Alavi, 2007; Berberian and Berberian, 1981; Stöcklin, 1968). Despite protracted and presumably continuous subduction along the northern Neotethyan margin for most of the Mesozoic and Cenozoic, arc volcanism across the UDMA appears to be dominated by an Eocene pulse or "flare-up" stage (Alavi, 1994; Berberian and King, 1981; Omrani et al., 2008; Verdel et al., 2011). More specifically, Verdel et al. (2011) argued that the pulse lasted for ~17 m.y. (from 55 to 37 Ma), ~10% of the total duration of the arc magmatism.

The SSZ, a belt of ~1500 km long and 150–250 km wide (Fig. 1), lies south of the UDMA and locates between the towns of Sanandaj/Urumieh in the northwest and Sirjan/Esfandaghen in the southeast (Alavi, 1994; Mohajjel and Fergusson, 2000; Mohajjel et al., 2003; Stöcklin, 1968). It is composed mainly of metamorphosed and complexly deformed rocks, associated with deformed/undeformed plutons and Mesozoic volcanic rocks (Mohajjel et al., 2003). In the SSZ, latest Neoproterozoic to Early Cambrian (~590–500 Ma) zircon U–Pb ages have been reported for granitoids and metamorphic rocks in localities (e.g., Azizi et al., 2011a; Hassanzadeh et al., 2008). These, along with coeval rocks identified from the Alborz and Central Iran (Fig. 1), are among the oldest rocks in Iran whose origins may be linked to the northern margin of Gondwanaland (Hassanzadeh et al., 2008).

It is generally consented that the Neotethyan subduction started in Iran from the Triassic (Arvin et al., 2007; Bagheri and Stampfli, 2008; Berberian and Berberian, 1981; Wilmsen et al., 2009). The timing of its ending, or, in other sense, onset of the Arabia–Eurasia collision, however, has long been a subject of debate, ranging from the Late Cretaceous (Alavi, 1994; Berberian and King, 1981), to the Late Paleocene or Early Eocene (Mazhari et al., 2009), the Eocene–Oligocene (Agard et al., 2005; Allen and Armstrong, 2008; Dargahi et al., 2010; Horton et al., 2008; Vincent et al., 2005), or even to the Middle Miocene–Pliocene (Axen et al., 2001; Azizi and Moinevaziri, 2009; Berberian and Berberian, 1981; Guest et al., 2006; McQuarrie et al., 2003; Okay et al., 2010; Stöcklin, 1968). More recently, Ballato et al. (2011) proposed a two-stage collision model that involves an initial collision in the Late Eocene and an acceleration of the regional deformation in the Early Miocene. Verdel et al. (2011) proposed a four-stage model with an emphasis on the Eocene magmatic flare-up that has been ascribed to the rollback of the Neotethyan slab after a flat slab subduction during Cretaceous time. Agard et al. (2011) published a comprehensive review that addresses the critical role played by the Neotethyan subduction throughout the Zagros orogeny in this "tectonic crossroad" region of the Alpine–Himalayan belt.

3. Samples and analytical methods

This study that focuses on the UDMA is a major component of the detailed geochronological and geochemical studies of the magmatic evolution in Iran conducted by our team. The UDMA is divided, from northwest to southeast, into three segments that we term Northwest, Central and Southeast parts, respectively, of the UDMA (Figs. 2–4). Among 150+ samples collected from the UDMA, a total of 56 volcanic and intrusive rocks of the UDMA were subjected to dating analyses. These include 46 samples selected for zircon U–Pb dating and 12 volcanic (mostly basaltic and andesitic) samples for Ar–Ar dating, the latter were chosen because of lacking zircon (basalts) or double-checking (andesites). Also, four granitoids collected from different parts of the SSZ were dated by using the zircon U–Pb method. Photos of field occurrence and thin sections of representative samples are given in Fig. 5 and Fig. A1, respectively. Zircon separations were performed via conventional methods combining heavy-liquid and magnetic separation techniques. Zircon separates were mounted by using epoxy and were measured for U–Pb ages by using the laser ablation-inductively coupled plasma mass spectrometry (LA-ICPMS) following the procedures described by Chiu et al. (2009).

Cathodoluminescence (CL) images (Fig. A2) were taken at the Institute of Earth Sciences, Academia Sinica, Taipei for examining the internal structures of individual zircon grains and selecting suitable positions for U–Pb analyses. Most zircons are euhedral and show long to short prismatic forms, with average crystal lengths of 100–200 μm and 150–250 μm for volcanic and intrusive rocks, respectively, and length-to-width ratios from 2:1 to 3:1. Most zircons are transparent, colorless to slightly brown and show oscillatory zoning indicative of magmatic origin (Hoskin and Schaltegger, 2003). Zircons with rounded or ovoid shape and complex internal textures are rare. Zircon U–Pb isotopic analyses were performed by using an Agilent 7500s ICP-MS coupled with a New Wave UP213 laser ablation system equipped at the Department of Geosciences, National Taiwan University. A spot size of 30 μm with laser repetition rate of 4 Hz was applied to all analyses, and the laser energy density was ~15 J/cm^2. Calibration was performed by using the zircon standard GJ-1 with a $^{207}Pb/^{206}Pb$ age of 608.5 ± 0.4 Ma (Jackson et al., 2004). Two well-known zircon standards 91500 and Mud Tank, together with a new zircon standard Plešovice (337.1 ± 0.4 Ma; Sláma et al., 2008), were used for data quality control. Measured U–Th–Pb isotope ratios were calculated by using the GLITTER 4.4 (GEMOC) software and the relative standard deviations of reference values for GJ-1 were set at 2%. The common lead was directly corrected by using the common lead correction function proposed by Anderson (2002), and the weighted mean U–Pb ages and concordia plots were carried out using by Isoplot v. 3.0 (Ludwig, 2003). Given that precise age measurements using $^{207}Pb/^{235}U$ and $^{207}Pb/^{206}Pb$ ratios are feasible usually only for Precambrian zircons (cf. Ireland and Williams, 2003), the weighted mean of pooled $^{206}Pb/^{238}U$ ages are taken to indicate the crystallization ages of the samples in this study.

4. Analytical results

Zircon age results are presented in four concordia diagrams (Figs. 6–9) and summarized, together with 12 whole-rock Ar–Ar ages, in Table 1. A detailed LA-ICP-MS dataset is given in Table A2, including zircon U–Pb isotope data of the 50 dated rock samples and a total of 981 individual zircon analyses. As shown in Figs. 6–9, all the mean ages are $^{206}Pb/^{238}U$ ages given at 95% confidence level, i.e., 2σ analytical uncertainties, coupled with mean square weighted deviations (MSWD). Magmatic ages obtained in this study appear to range from 166.8 ± 1.7 Ma to 5.3 ± 0.1 Ma in the UDMA, and from 175.2 ± 1.8 Ma to 163.9 ± 1.8 Ma in the SSZ. In addition to the magmatic zircons, inherited zircons of older U–Pb ages are occasionally detected, and exceptionally abundant in two basaltic rocks (Figs. 6c

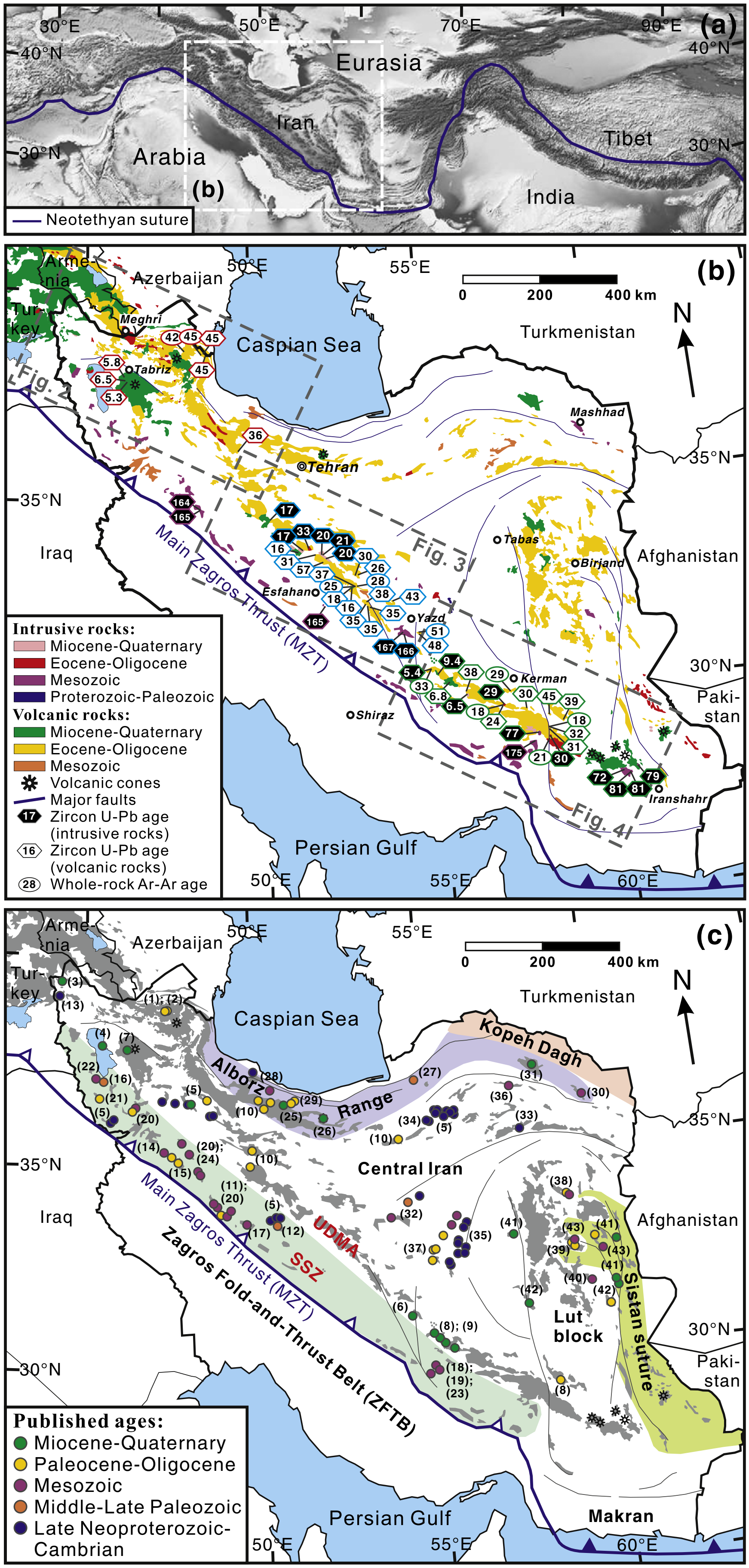
(a)
30°E
50°E
70°E
90°E
40°N
30°N
Eurasia
Iran
Arabia
Tibet
India
(b)
Neotethyan suture
(b)
Arme-nia
Azerbaijan
Tur-key
Caspian Sea
Turkmenistan
50°E
55°E
0 200 400 km
N
Meghri
Tabriz
Tehran
Mashhad
Tabas
Birjand
Esfahan
Yazd
Kerman
Shiraz
Iranshahr
Iraq
Afghanistan
Paki-stan
Persian Gulf
Main Zagros Thrust (MZT)
Fig. 2
Fig. 3
Fig. 4
35°N
30°N
60°E
Intrusive rocks:
Miocene-Quaternary
Eocene-Oligocene
Mesozoic
Proterozoic-Paleozoic
Volcanic rocks:
Miocene-Quaternary
Eocene-Oligocene
Mesozoic
Volcanic cones
Major faults
Zircon U-Pb age (intrusive rocks)
Zircon U-Pb age (volcanic rocks)
Whole-rock Ar-Ar age
(c)
Arme-nia
Azerbaijan
Tur-key
Caspian Sea
Turkmenistan
Kopeh Dagh
Alborz Range
Central Iran
UDMA
SSZ
Main Zagros Thrust (MZT)
Zagros Fold-and-Thrust Belt (ZFTB)
Lut block
Sistan suture
Makran
Iraq
Afghanistan
Paki-stan
Persian Gulf
50°E
55°E
60°E
35°N
30°N
0 200 400 km
N
Published ages:
Miocene-Quaternary
Paleocene-Oligocene
Mesozoic
Middle-Late Paleozoic
Late Neoproterozoic-Cambrian

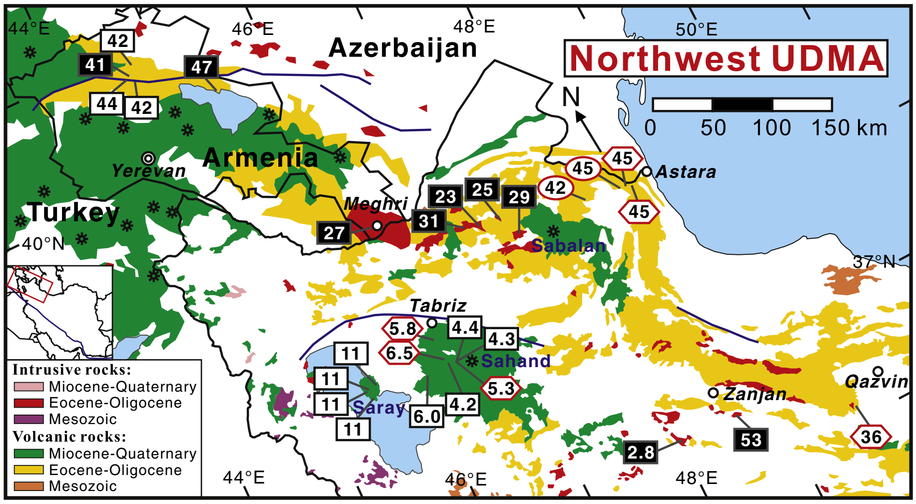

Fig. 2. Simplified geological map of the Northwest UDMA and Armenia showing sample localities of this study and the literature age data. The latter, shown within squares, are from Hassanzadeh et al. (2008), Aghazadeh et al. (2010), Chiu et al. (2010), Aghazadeh et al. (2011) and Lin (2011). Symbols of our new ages are the same as in Fig. 1.

and 7i; Table A2), which require a cautious explanation (see below). Here we present our results obtained from the UDMA and SSZ together with available literature age data. Based on the 1/2,500,000 geological map and 1/250,000 quadrangle maps of Iran (published by the Geological Survey of Iran), Cenozoic volcanic successions have been regarded dominantly as Eocene in ages. However, our results identify a significant number of Oligocene and Miocene ages from the presumed Eocene volcanic sequences on the geological maps, particularly in the Southeast UDMA (see remarks in Table 1). For example, a Late Oligocene age of 23.6 ± 0.4 Ma is obtained from an andesite 10-IR-ZS-74 sampled from the Middle Eocene volcanic succession "E^{V}_{3}" on the 1/250,000 geological quadrangle map of "Sirjan" area (Hosseini et al., 1995). Our new age data hence point to the necessity of carefully reevaluating the age distribution of Cenozoic volcanic successions in Iran.

4.1. Northwest UDMA

In the northwestern part of the UDMA in Iran (Fig. 2), our fieldwork and sampling were hampered by two complications: (1) the widespread occurrence of Miocene to Quaternary volcanic rocks around two large volcanoes, Sahand and Sabalan, and (2) its merge with the western Alborz. Judging from our work in Armenia and the easternmost part of Anatolia (Lin, 2011; Lin et al., 2011; see below for more detail), where calc-alkaline magmatic rocks of Eocene to Early Oligocene ages are observed, we regard this part of the UDMA in a broader sense and thus include Armenia and the Sabalan–Qazvin areas, despite that workers commonly consider the latter "strictly" as part of the Alborz Range (e.g., Aghazadeh et al., 2010, 2011; Alavi, 1994; Omrani et al., 2008).

4.1.1. Sabalan–Astara areas

The ages of four basaltic samples from this region were obtained. Two of them which were recovered near the national border between Iran and Azerbaijan yielded coeval zircon U–Pb ages of ~45 Ma (Fig. 6; a and b). Both samples contain many older zircons (Table A2), suggesting crustal contamination in the petrogenesis. In particular, sample 08-IR-ZS-87 has exceptionally abundant inherited zircons that gave a mean $^{206}Pb/^{238}U$ age of 232.8 ± 3.3 Ma (Fig. 6c), implying the presence of a major contaminant or crustal host rock that formed in the Early Triassic related perhaps to the Paleotethys evolution in the region (e.g., Karimpour et al., 2010). It is speculated that even the Eocene zircons are not "real" magmatic zircons (i.e., crystallizing from the basaltic melts) but, instead, were captured from broadly coeval and more evolved magmas. To confirm the Eocene ages, two basaltic samples from nearby areas were dated by using the Ar–Ar method that gave generally agreeing plateau ages at 42.1 ± 0.3 and 44.5 ± 0.2 Ma, respectively (Table 1).

Vincent et al. (2005) have published similar Ar–Ar ages of 41–38 Ma for four basalts and an andesite within the volcanic succession from the Talysh in the Azerbaijan territory. More literature age data are available from the Khankandi pluton around the Sabalan volcano (Fig. 2), where Aghazadeh et al. (2010) reported a zircon U–Pb age of 28.9 ± 1.1 Ma, averaged from two age peaks of about 33.3 Ma and 27.9 Ma, for a monzonite sample. Later, Aghazadeh et al. (2011) reported additional zircon U–Pb ages of ~31–23 Ma for three granitioids of shoshonitic geochemical features from the Shaivar Dagh plutonic complex (Fig. 2 and Table A1). These Oligocene ages are younger than our Eocene results above-described, but corresponding to those we obtained from the adjacent Meghri plutonic complex that crops out in SE Armenia or across the national border (see below).

4.1.2. Zanjan–Qazvin areas

Only one sample was dated here. A basaltic andesite (08-IR-ZS-46) from the southwest of Qazvin yielded zircon U–Pb age of 35.8 ± 0.3 Ma in the Late Eocene (Fig. 6d). In the south of Zanjan (Fig. 2), a granite from the Soltanieh Mountains has been dated by

Fig. 1. (a–b) Simplified geological map showing sample localities and distribution of magmatic rocks in Iran (after 1/2,500,000 geological map of Iran, Geological Survey of Iran). New age results reported in this paper from the UDMA and SSZ are given in parentheses (number in Ma). (c) Published magmatic ages in Iran; data sources including (1) Aghazadeh et al. (2010), (2) Aghazadeh et al. (2011), (3) Allen et al. (2011), (4) Chiu et al. (2010), (5) Hassanzadeh et al. (2008), (6) Kouhestani et al. (2012), (7) Lin (2011), (8) McInnes et al. (2003), (9) McInnes et al. (2005), (10) Verdel et al. (2011), (11) Ahmadi Khalaji et al. (2007), (12) Alirezaei and Hassanzadeh (2012), (13) Azizi et al. (2011a), (14) Azizi et al. (2011b), (15) Azizi et al. (2011c), (16) Bea et al. (2011), (17) Esna-Ashari et al. (2012), (18) Fazlnia et al. (2007), (19) Fazlnia et al. (2009), (20) Mahmoudi et al. (2011), (21) Mazhari et al. (2009), (22) Mazhari et al. (2011), (23) Mousivand et al. (2011), (24) Shahbazi et al. (2010), (25) Axen et al. (2001), (26) Davidson et al. (2004), (27) Ghavidel-Syooki et al. (2011), (28) Guest et al. (2006), (29) Horton et al. (2008), (30) Karimpour et al. (2010), (31) Shabanian et al. (2009), (32) Bagheri and Stampfli (2008), (33) Karimpour et al. (2011a), (34) Rahmati-Ilkhchi et al. (2011), (35) Ramezani and Tucker (2003), (36) Rossetti et al. (2010), (37) Verdel et al. (2007), (38) Karimpour et al. (2011b), (39) Malekzadeh et al. (2010), (40) Mahmoudi et al. (2010), (41) Pang et al. (2012), (42) Walker et al. (2009), and (43) Zarrinkoub et al. (2012). Details regarding published ages are given in Table A1.

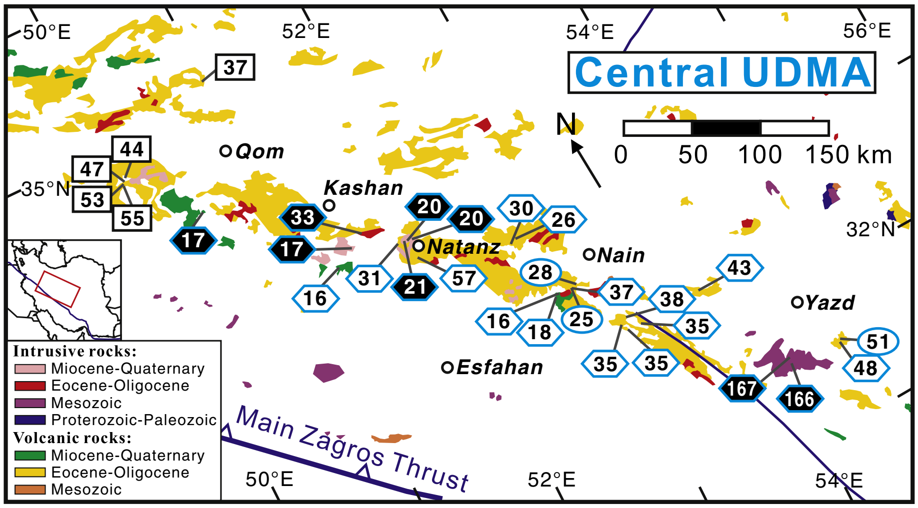

Fig. 3. Simplified geological map of the Central UDMA showing sample localities of this study and the literature data. The latter are from Verdel et al. (2011). Age symbols are the same as in the previous figure.

Hassanzadeh et al. (2008), yielding an older zircon U–Pb age of 53.4 ± 0.3 Ma in the Early Eocene (Table A1). In addition, Hassanzadeh et al. (2008) documented a Pliocene (2.8 Ma) age for a leucogranite in the area (Fig. 2) and interpreted it as the magmatic product postdating the Arabia–Eurasia collision.

4.1.3. Armenia

The Eocene–Oligocene magmatic rocks exposed in Armenia (Figs. 1 and 2) are regarded as an extension of the Northwest UDMA. In a thesis work, Lin (2011) carried out six zircon U–Pb ages of about 47–27 Ma and four whole-rock Ar–Ar ages of about 57–41 Ma for these rocks, with the former plotting in Fig. 2. They are typical calc-alkaline rocks geochemically comparable to those from the Central and Southeast UDMA, and elsewhere of the continental arcs (Tatsumi and Eggins, 1995). In addition to a granite sample RAF-1 dated at ~27 Ma (Lin, 2011), six more granitoids from the Meghri plutonic complex (Fig. 2) have been dated in a detailed study by our team and yielded zircon U–Pb ages of about 46–22 Ma; these rocks, moreover, exhibit a significant change in geochemical characteristics from calc-alkaline to adakitic (S.-L. Chung et al., unpubl. data). In Armenia, the magmatism that lasted from the latest Paleocene to the latest Oligocene appears to have been active semi-continuously. These age data will be included for discussion in the following sections.

4.1.4. Post-collisional volcanism

The youngest magmatic rocks in the Northwest UDMA occur in the Sahand and Sabalan volcanoes that have long been attributed to a "post-collisional" tectonic setting (e.g., Şengör and Kidd, 1978). Here we adopt the term "post-collisional", despite that the collision continues, as the magmatism apparently postdates onset of the collision and has little or nothing to do with collisional contraction, or even affiliates with additional mechanism such as extension. In Sahand (Fig. 2), three andesitic ignimbrites (SiO_2 = 54–64 wt.%) dated by the zircon U–Pb method yielded Late Miocene ages of 6.5–5.3 Ma (Fig. 6; e–g; Table A2). The results are in good accordance with the whole-rock Ar–Ar ages of 6.0–4.3 Ma obtained from four other andesites (Table A1; Lin, 2011). The Sabalan volcano (Fig. 2) consists largely of Quaternary eruptions, as evidenced by an unpublished zircon U–Pb age as young as ~0.4 Ma measured by the secondary ion mass spectrometry equipped at the Institute of Geology and Geophysics, Chinese Academy of Sciences, Beijing (Li et al., 2009). Quaternary Ar–Ar ages (ca. 1.87 to 0.40 Ma) have also been

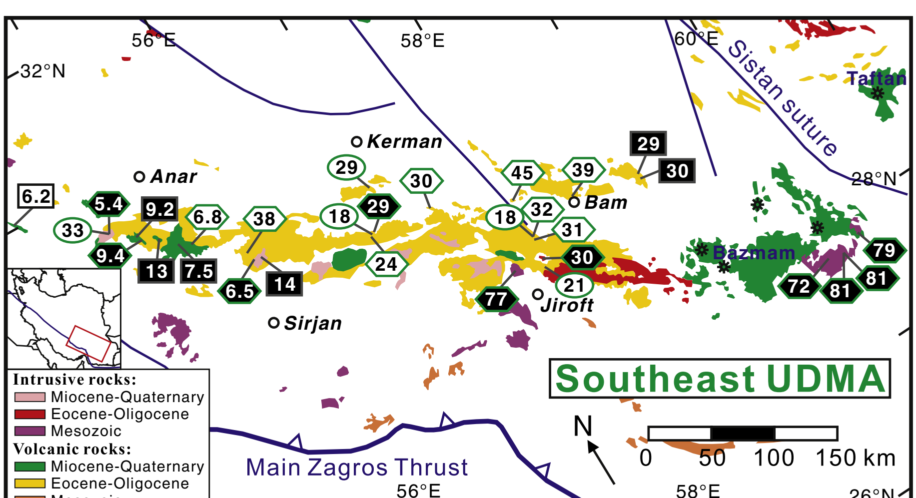

Fig. 4. Simplified geological map of the Southeast UDMA showing sample localities of this study and the literature data. The latter are from McInnes et al. (2003, 2005) and Kouhestani et al. (2012). Age symbols are the same as in the previous figure.

Fig. 5. Selected outcrop photos from (a) the Northwest UDMA, (b–d) the Central UDMA, (e–g) the Southeast UDMA, and (h) the SSZ.

reported for basaltic lavas in the Maku region of NW Iran (Allen et al., 2011). In Saray, a volcanic dome east off the Urumieh Lake (Fig. 2) and composed mainly of high-K basaltic lavas, Ar–Ar ages of ~11 Ma were obtained for the four samples (Table A1; Chiu et al., 2010; Pang et al., in review). This age corresponds to the onset timing of the extensive volcanism postdating the Arabia–Eurasia collision and spreading over much of the Lesser Caucasus, NW Iran and eastern Anatolia regions (e.g., Keskin, 2003; Lin, 2011; Lin et al., 2011).

4.2. Central UDMA

A total of 25 samples from the central part of the UDMA (Fig. 3) were dated and they yielded two distinctive age intervals of ~166 Ma in the Middle Jurassic and of ~57–16 Ma from the latest Paleocene to the Middle Miocene (Table 1 and Fig. 7).

4.2.1. Qom–Kashan–Natanz areas

Nine samples were dated from this part. A granodiorite (10-IR-ZS-106; Table 1) from a small intrusion southwest of Qom, gave a latest Early Miocene age of 17.4 ± 0.2 Ma (Fig. 7a). However, in the 1/250,000 geological quadrangle map of the "Qom" area (Emami, 1981), this granodiorite body was mapped as the youngest intrusive phase in the region and given a post-Miocene age, which mismatches our dating result. Therefore, the reliability of the Miocene to Pliocene ages given also for neighboring young volcanic rocks in the map is questionable. Between Kashan and Natanz, four samples including two andesites and two diorites yielded zircon U–Pb ages of 33–16 Ma from the Early Oligocene to the Middle Miocene (Fig. 7; b–e). In the Natanz area, three granitoids gave nearly identical Early Miocene ages from 21.2 ± 0.3 to 19.6 ± 0.3 Ma (Fig. 7; f–g and j), and a basalt gave a latest Paleocene age of 56.5 ± 2.6 Ma based on four laser spots of three zircon grains (Fig. 7 h

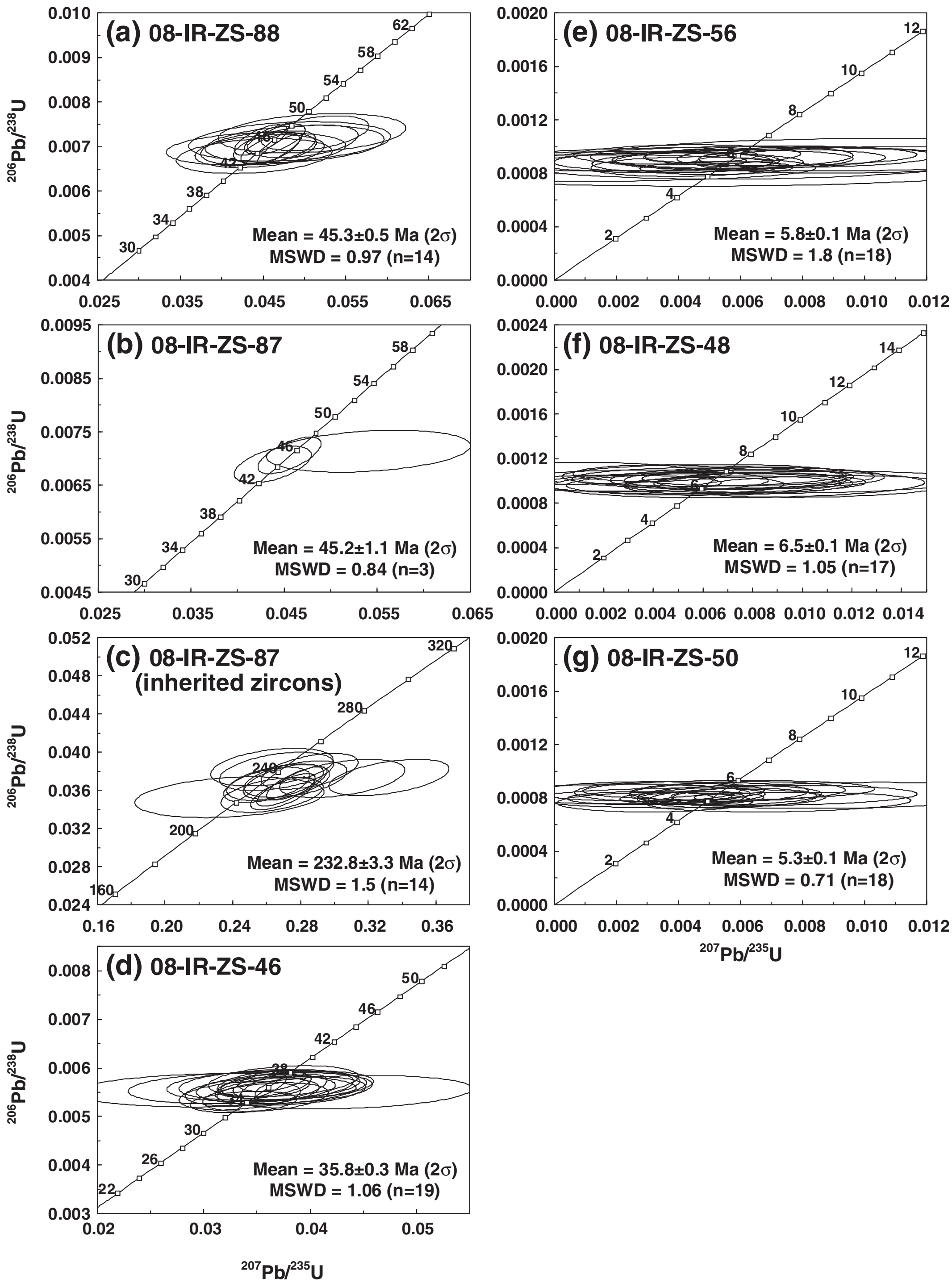

Fig. 6. Concordia diagrams of zircon U–Pb age results of magmatic rocks form the Northwest UDMA. "Mean" values of each sample are $^{206}Pb/^{238}U$ ages in Ma.

and Table A2). This basalt sample, moreover, contains abundant inherited zircons that gave a much older U–Pb age cluster at 278.2 ± 2.9 Ma (Fig. 7i), suggesting a contamination of such crustal rocks in the petrogenesis. A slightly younger Middle Permian age (262 ± 1 Ma) has been reported by Bagheri and Stampfli (2008) for a trondhjemite complex in Central Iran (Table A1), ~180 km east of this basalt outcrop. Recently, the volcanic and sedimentary strata in the northwest and the north of Qom have been studied by Verdel et al. (2011) who gave four zircon U–Pb ages of about 55–44 Ma from three different andesitic sections in the Tafresh area and an age of 37.3 ± 1.2 Ma from a tuff in the Saveh area (Table A1).

4.2.2. Nain area

From this area, seven volcanic samples were dated. Five of them were collected along the highway between Nain and Esfahan (Fig. 3), and yielded three zircon U–Pb ages of 37.0 ± 0.4 Ma in the latest Eocene (Fig. 7o) and of ~18–16 Ma in the Miocene (Fig. 7; k–l), and other two Ar–Ar ages of 27.9 ± 0.4 and 25.0 ± 0.4 Ma in the Late Oligocene (Table 1). The remaining two samples are ignimbrite and andesite from the northwest of Nain (Fig. 3), both of which gave Oligocene ages of 30.1 ± 0.9 and 26.3 ± 0.4 Ma (Fig. 7; m–n). Note that two samples (10-IR-ZS-100 and -101) were dated doubly by zircon U–Pb and whole rock Ar–Ar methods and yielded consistent age results (Table 1).

4.2.3. Nain–Yazd areas

Nine samples dated were from this region. Beside the Batlaq-e-Gavkhuni salt marsh, three andesites sampled from different volcanic domes yielded identical Late Eocene ages of ~35 Ma and a black tuff gave a similar age of 37.8 ± 0.6 Ma (Fig. 7; p–s). A Middle Eocene age of 42.9 ± 0.4 Ma (Fig. 7t) was obtained by an andesite from ~80 km southeast of Nain (Fig. 3). Southwest of Yazd, a granodiorite and a diorite sampled from the Shir–Kuh pluton yielded Middle Jurassic ages of 166.1 ± 1.5 and 166.8 ± 1.7 Ma (Fig. 7; u–v). Besides, two andesite flows from the nearby Mehriz area gave a zircon U–Pb age of 47.8 ± 1.2 Ma (Fig. 7w) and an Ar–Ar age of 51.4 ± 0.4 Ma (08-IR-ZS-17; Table 1). Note that the former is the only outcrop within the UDMA from which Jurassic magmatic rocks have been identified. Four inherited zircon grains of ~1.8 Ga were detected in the

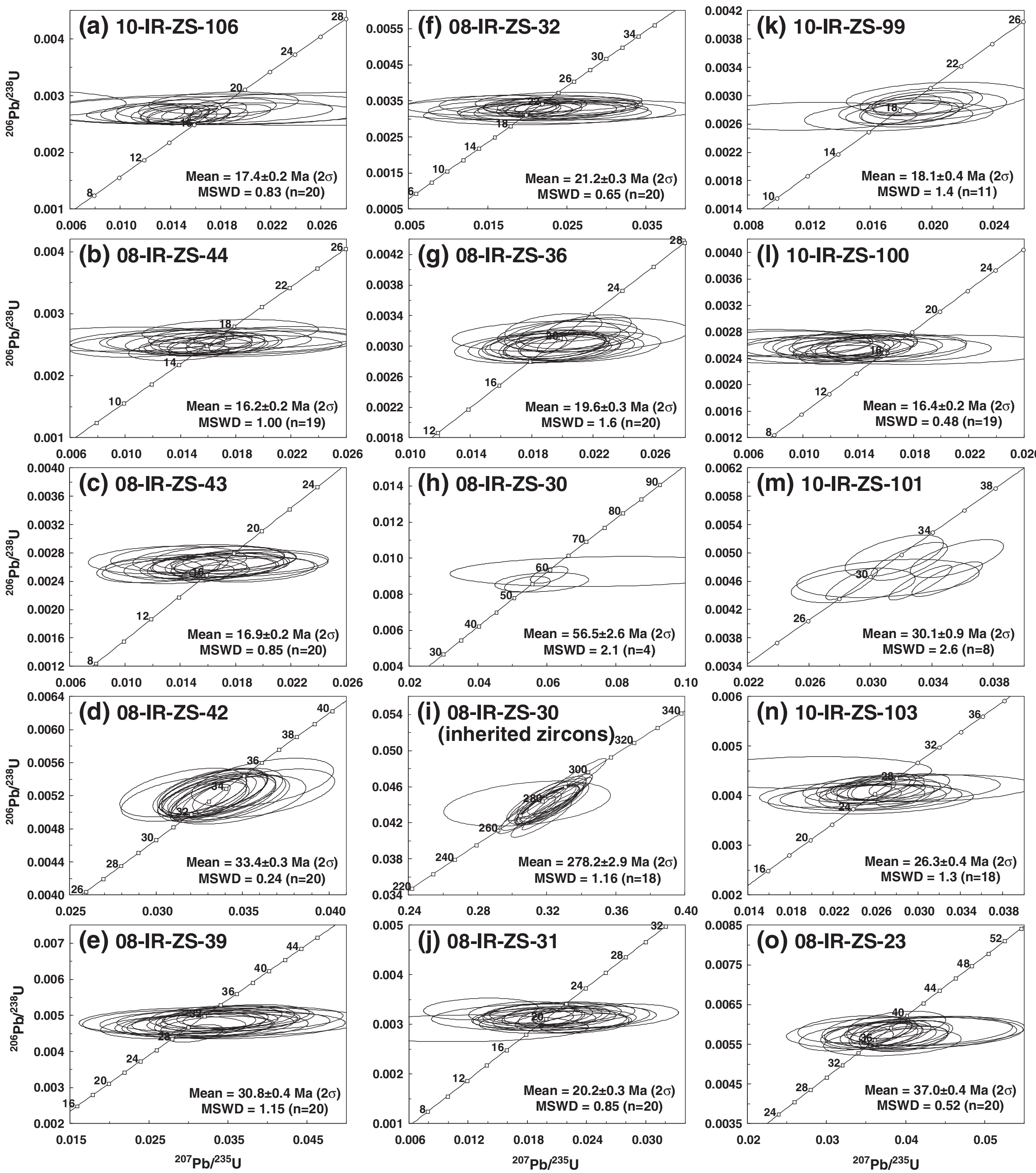

Fig. 7. Concordia diagrams of zircon U–Pb age results of magmatic rocks form the Central UDMA. "Mean" values of each sample are $^{206}Pb/^{238}U$ ages in Ma.

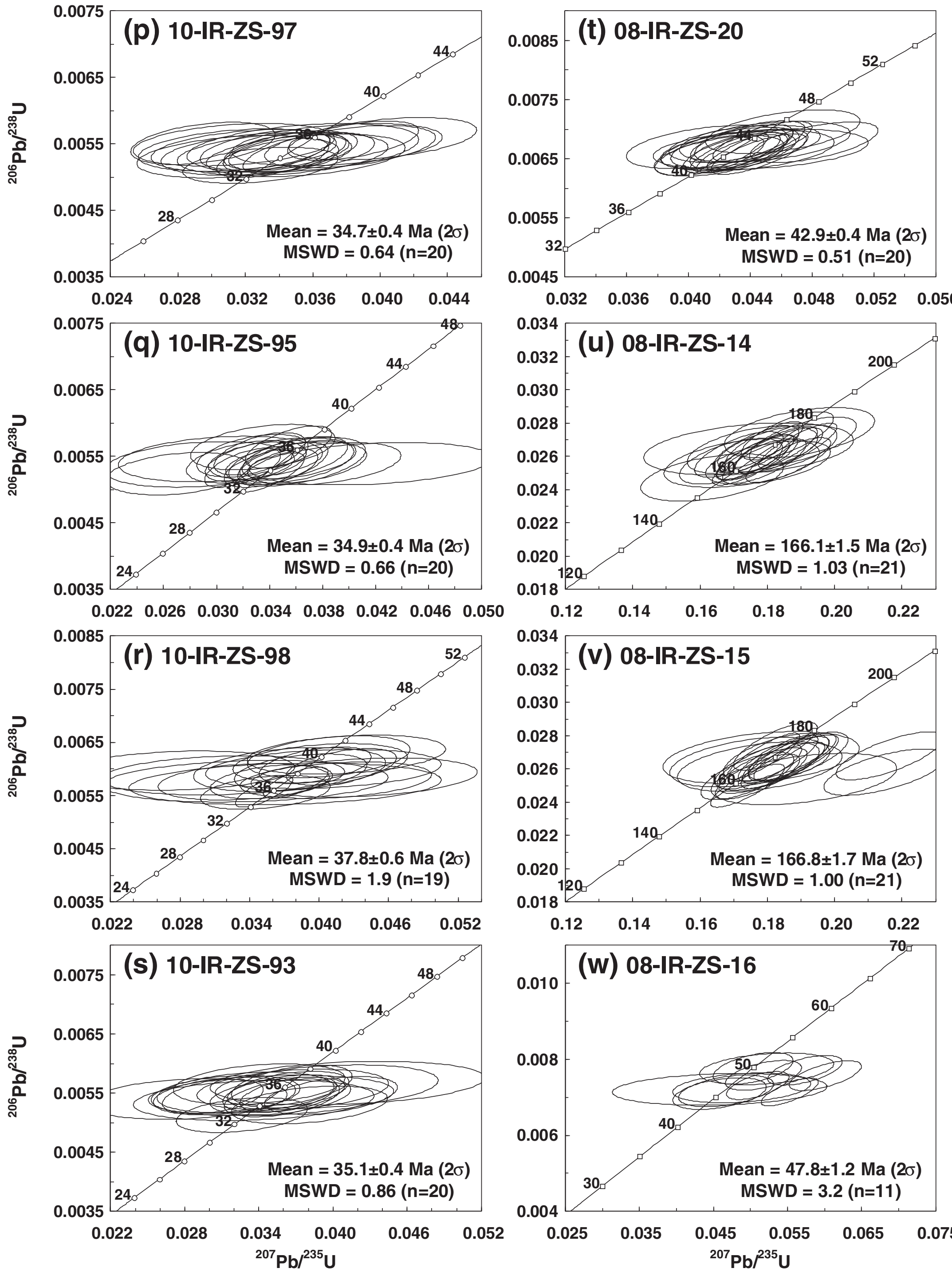

Fig. 7 (*continued*).

granodiorite sample 08-IR-ZS-14 (Table A2). The Shir–Kuh pluton, composed mainly of granodioritic to granitic rocks, has been known to be Jurassic based on the Rb–Sr and K–Ar dating results of ~186–159 Ma and field observations that it intrudes Early Jurassic sandstones and is overlain by Cretaceous limestone (Sheibi et al., 2010; and references therein).

4.3. Southeast UDMA

A total of 18 dated samples were from this part of the UDMA (Fig. 4), yielding two age intervals of ~81–72 Ma in the Late Cretaceous and of ~45–6 Ma during Middle Eocene and latest Miocene time (Table 1 and Fig. 8). We reiterate the drawback of the geological maps that many volcanic units mapped as Eocene are actually of Oligocene or Miocene ages.

4.3.1. Anar–Sirjan–Kerman areas

Eleven samples dated were from this part. Four of them sampled between Anar and Sirjan gave Late Miocene ages of ~10–6 Ma (Fig. 8; a–c and e), among the youngest magmatic ages obtained from the entire UDMA. We note that McInnes et al. (2003, 2005) reported zircon U–Pb ages for the Kuh Panj granitoids that host ore

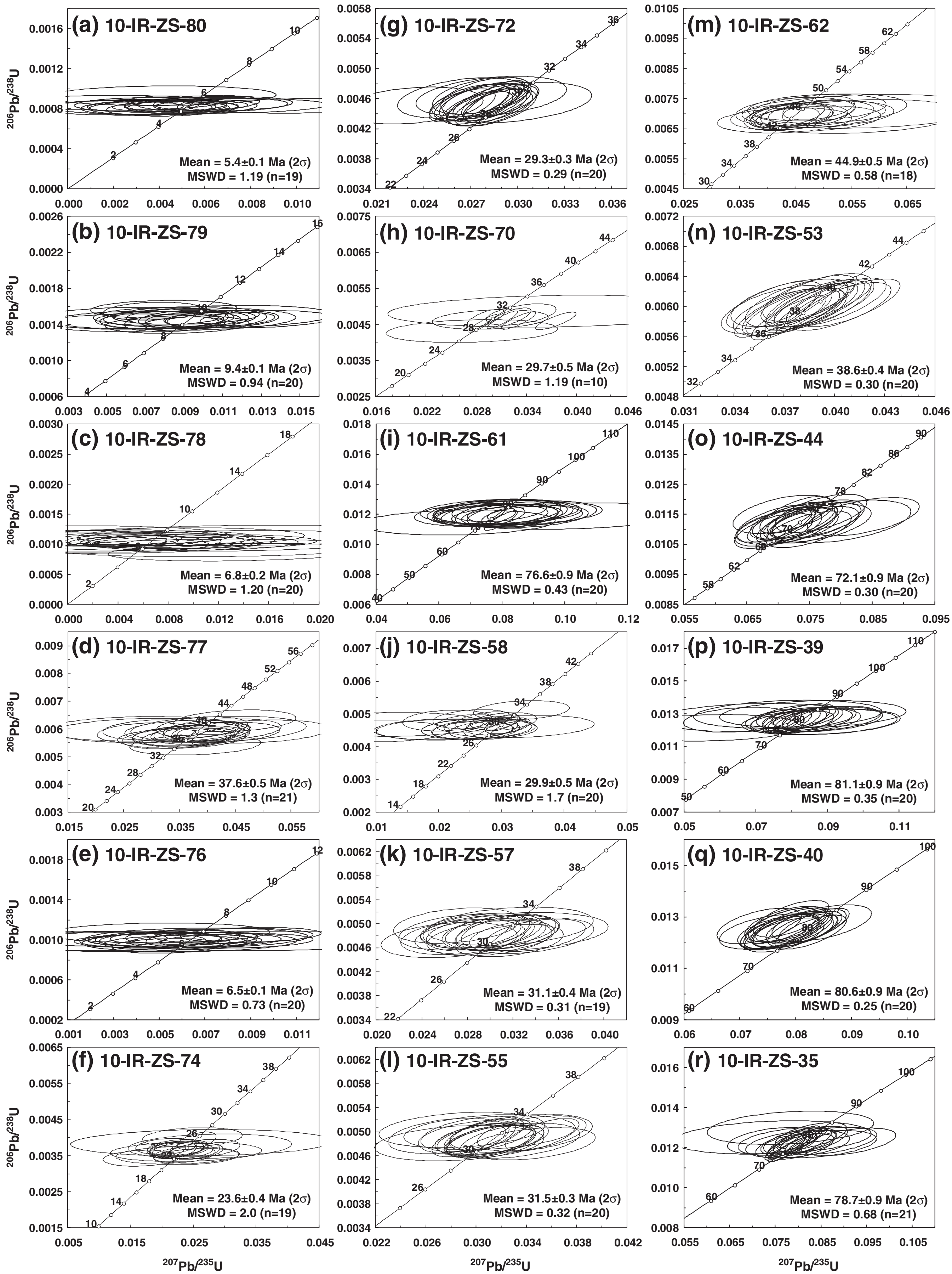

Fig. 8. Concordia diagrams of zircon U–Pb age results of magmatic rocks form the Southeast UDMA. "Mean" values of each sample are $^{206}Pb/^{238}U$ ages in Ma.

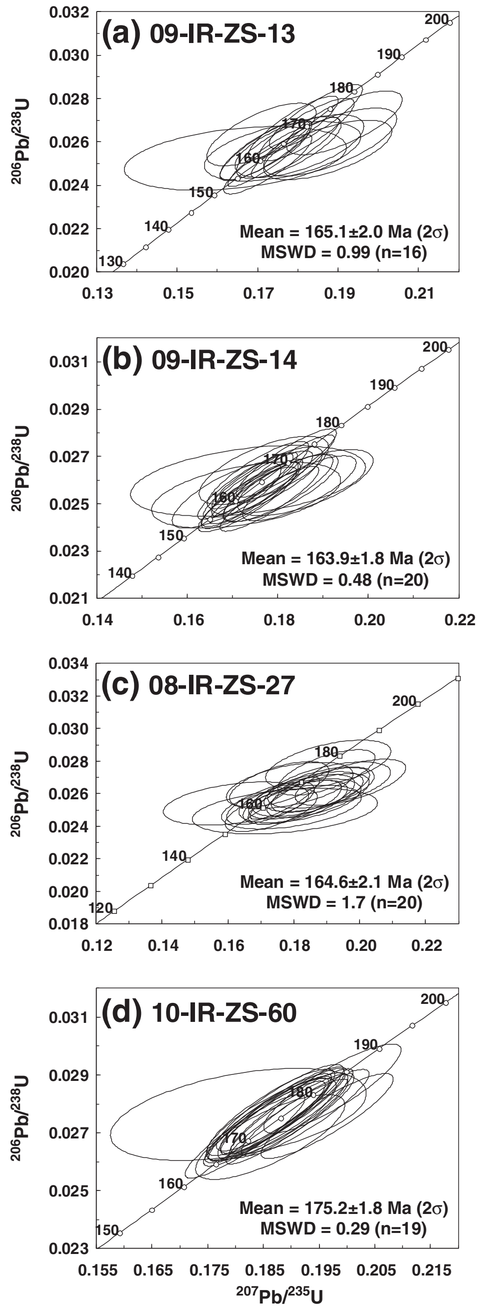

Fig. 9. Concordia diagrams of zircon U–Pb age results of magmatic rocks form the SSZ. "Mean" values of each sample are $^{206}Pb/^{238}U$ ages in Ma.

deposits; these include 13.6 ± 0.1 Ma from Sarcheshmeh, 12.5 ± 0.1 Ma from Meiduk, 9.2 ± 0.1 Ma from Iju and 7.5 ± 0.1 Ma from Abdar areas (Fig. 4 and Table A1), which appear in general consistency with our results. Kouhestani et al. (2012) recently documented a Late Miocene age of 6.2 ± 0.2 Ma for the Chah Zard volcanic complex, ~100 km southwest of Anar (Fig. 4). A Late Eocene age of 37.6 ± 0.5 Ma (Fig. 8d) was obtained for an andesitic lava cut by the Sarcheshmeh road, ~50 km north of the Sirjan township (Fig. 4). South of Kerman, Oligocene ages of ~30–24 Ma were given by three other samples that are two andesite flows and a diorite (Fig. 8; f–h). Additionally, three basalts yielded Oligocene to Middle Miocene Ar–Ar ages of 32.5 ± 0.2, 29.0 ± 0.2 and 17.6 ± 0.1 Ma, respectively (Table 1).

4.3.2. Bam–Jiroft areas

Eight ages were obtained from this part. A Late Cretaceous zircon U–Pb age of 76.6 ± 0.9 Ma (Fig. 8i) was given by a gabbro from Jiroft area (Fig. 4). Three Oligocene ages, 29.9 ± 0.5, 31.1 ± 0.4 and 31.5 ± 0.3 Ma, respectively (Fig. 8; j–l), were obtained by a diorite, a rhyolite and a green tuff near Jebalbarez. North of Bam, two andesitic lavas gave Eocene ages of 44.9 ± 0.5 and 38.6 ± 0.4 Ma (Fig. 8; m–n). We note that two Oligocene ages, 29.3 ± 0.2 and 29.7 ± 0.3 Ma, have also been reported by McInnes et al. (2003) from the Rigan granitoids that crop out near Bam (Fig. 4 and Table A1). Early Miocene Ar–Ar ages of ~20–18 Ma were obtained by a basalt and a rhyolite in this region (Table 1).

4.3.3. Bazman area

All of the four dated intrusive rocks (46–71 wt.% of SiO_2) from this area (Table 1) yielded Late Cretaceous ages of ~81–72 Ma (Fig. 8; o–r). This Late Cretaceous age has been argued since Berberian et al. (1982), who reported a similar age of 74.2 ± 2.0 Ma from the diorite to the granite complex using the Rb–Sr whole-rock isochron method, have been considered unreliable. Our data, therefore, stand up as the first compelling evidence for the existence of Late Cretaceous igneous activity in this region. We note also that four inherited zircons of Middle Jurassic ages (~168–162 Ma; Table A2) are present in the most silicic granite sample 10-IR-ZS-35 (SiO_2 = 71 wt.%; Table 1).

4.4. The SSZ

Four granite samples from the SSZ were dated in this study and all yielded Jurassic ages (Table 1 and Fig. 9). Two of them from the Alvand plutonic complex (nearby Hamadan) gave zircon U–Pb ages of 165.1 ± 2.0 and 163.9 ± 1.8 Ma (Fig. 9; a–b). The other two granites were from Kolah Ghazi area in the south of Esfahan and from Sargaz in the west of Jiroft, which yielded U–Pb ages of 164.6 ± 2.1 and 175.2 ± 1.8 Ma, respectively (Fig. 9; c–d). There are ten grains of older zircons aged from ca. 2500 to 220 Ma (Table A2) that were detected in the Alvand samples.

Several complexes in the SSZ have been recently well dated by using the zircon U–Pb method and mostly yielded Middle–Late Jurassic ages. These data, listed from the northwest to the southeast (Fig. 1b), include (1) the Gorveh plutonic complex (157–149 Ma; Mahmoudi et al., 2011); (2) the Suffi abad granitoids (149–144 Ma; Azizi et al., 2011b); (3) the Alvand plutonic complex (167–153 Ma; Mahmoudi et al., 2011; Shahbazi et al., 2010); (4) the Boroujerd granitoids (172–169 Ma; Ahmadi Khalaji et al., 2007; Mahmoudi et al., 2011); (5) the Astaneh pluton (168 ± 1 Ma; Mahmoudi et al., 2011); (6) the Chah–Dozdan Batholith (173–164 Ma; Fazlnia et al., 2007); (7) the Qori metamorphic complex (147 ± 1 Ma; Fazlnia et al., 2009); and (8) the Chahgaz volcanic complex (176–173 Ma; Mousivand et al., 2011). In addition, Cretaceous zircon U–Pb ages have been reported for a leucogranite from the Hasan Salary pluton (108.8 ± 0.3 Ma; Mahmoudi et al., 2011) and a diorite from the Naqadeh complex (96 ± 2.3 Ma; Mazhari et al., 2011). Also documented are small-volume exposures of Paleogene magmatic bodies in the northwestern SSZ that, based on the literature data so far (Fig. 1b), include (1) intrusive rocks of ~41 Ma from the Piranshahr massif (Mazhari et al., 2009), (2) granitoids of ~37–35 Ma from Taa–Baysaran and a basaltic rock of 54.6 ± 1.8 Ma from Kamyaran (Azizi et al., 2011c), and (3) a granite dated at 59.8 ± 0.2 Ma from the Hasan Salary pluton and a quartz monzodiorite at 34.9 ± 0.1 Ma from the Gosheh–Tavandasht complex (Mahmoudi et al., 2011). All the above literature data are listed in Table A1.

4.5. Inherited zircons

A total of 79 inherited ages were analyzed from 78 zircon grains (Table A2), including 68 grains from the UDMA and 10 others from

Table 1
Summary of zircon U–Pb and related age data of magmatic rocks from the UDMA and SSZ, Iran.

Sample	Locality	Longitude (°E)	Latitude (°N)	Elevation (m)	Rock type	SiO_2 (wt.%)[a]	Age	±2σ	Remarks[b]
a. Northwest UDMA									
08-IR-ZS-88	Sabalan-Astara	48.6586	38.3908	375	Basalt	51.33	45.3	0.5	
08-IR-ZS-87		48.5858	38.4394	1426	Basalt	49.58	45.2	1.1	
							232.8	3.3	
08-IR-ZS-79[a]		48.2233	38.4903	1513	Basalt	48.30	42.1	0.3	
08-IR-ZS-86[a]		48.4981	38.4161	1448	Basalt	50.57	44.5	0.2	
08-IR-ZS-46	Qazvin	49.6372	36.0650	1415	Basaltic andesite	54.32	35.8	0.3	
08-IR-ZS-56	Sahand	46.1894	37.8769	1808	Ignimbrite	62.93	5.8	0.1	
08-IR-ZS-48		46.2589	37.7850	2314	Andesite	54.32	6.5	0.1	
08-IR-ZS-50		46.2956	37.7644	2675	Ignimbrite	64.07	5.3	0.1	
b. Central UDMA									
10-IR-ZS-106	Qom	50.5108	34.3292	1298	Granodiorite	60.25	17.4	0.2	Post-Miocene (Qom)
08-IR-ZS-44	Kashan-Natanz	51.2683	33.6114	2456	Andesite	60.12	16.2	0.2	
08-IR-ZS-43		51.4222	33.6789	2241	Diorite	61.85	16.9	0.2	
08-IR-ZS-42		51.4986	33.7281	1869	Microdiorite	57.72	33.4	0.3	
08-IR-ZS-39		51.6183	33.5886	2120	Andesite	61.20	30.8	0.4	M.-L. Eocene (Kashan)
08-IR-ZS-32	Natanz	51.8444	33.5214	2082	Gabbro	47.98	21.2	0.3	
08-IR-ZS-36		51.8522	33.5147	2021	Granite	–	19.6	0.3	
08-IR-ZS-30		51.8747	33.3611	1853	Basalt	50.97	56.5	2.6	
							278.2	2.9	
08-IR-ZS-31		51.9219	33.4911	1727	Granodiorite	65.56	20.2	0.3	
10-IR-ZS-99	Nain	52.6728	32.7236	2055	Andesite	60.38	18.1	0.4	
10-IR-ZS-100		52.8056	32.7153	2417	Trachyandesite	61.33	16.4	0.2	
10-IR-ZS-100[a]							18.4	0.2	
10-IR-ZS-101		52.8183	33.0286	2027	Ignimbrite	65.69	30.1	0.9	E. Eocene (Anarak)
10-IR-ZS-101[a]							31.9	0.2	
10-IR-ZS-103		52.8672	33.0450	2148	Andesite	68.65	26.3	0.4	Eocene (Anarak)
08-IR-ZS-23		52.8814	32.7408	2211	Rhyolite	71.73	37.0	0.4	
08-IR-ZS-24[a]		52.8814	32.7408	2211	Andesite	68.99	25.0	0.4	Eocene (Nain)
08-IR-ZS-22[a]		52.9464	32.7622	1963	Andesite	63.47	27.9	0.4	Eocene (Nain)
10-IR-ZS-97	Nain-Yazd	53.0797	32.3008	1675	Trachyandesite	66.35	34.7	0.4	
10-IR-ZS-95		53.1014	32.2731	1748	Andesite	67.41	34.9	0.4	
10-IR-ZS-98		53.1100	32.3214	1684	Tuff	56.73	37.8	0.6	
10-IR-ZS-93		53.1761	32.2625	1854	Andesite	69.22	35.1	0.4	
08-IR-ZS-20		53.8414	32.3389	1166	Andesite	62.39	42.9	0.4	
08-IR-ZS-14	Yazd	54.1239	31.5922	2568	Granodiorite	67.72	166.1	1.5	
08-IR-ZS-15		54.1319	31.6258	2338	Diorite	53.52	166.8	1.7	
08-IR-ZS-16		54.4494	31.5278	1532	Andesite	59.47	47.8	1.2	
08-IR-ZS-17[a]		54.4519	31.5344	1517	Andesite	63.33	51.4	0.4	
c. Southeast UDMA									
10-IR-ZS-80	Anar-Sirjan	54.9211	30.5989	2578	Granodiorite	64.25	5.4	0.1	
10-IR-ZS-81[a]		54.9211	30.5989	2578	Basalt	47.63	32.5	0.2	
10-IR-ZS-79		55.0081	30.4744	2337	Granodiorite	62.46	9.4	0.1	
10-IR-ZS-78		55.3781	30.2319	2247	Ignimbrite	60.14	6.8	0.2	
10-IR-ZS-77		55.7128	30.0019	2332	Andesite	59.17	37.6	0.5	
10-IR-ZS-76		55.7153	29.9592	2376	Microdiorite	65.07	6.5	0.1	
10-IR-ZS-74	Kerman	56.7161	29.6358	2711	Andesite	57.69	23.6	0.4	M. Eocene (Sirjan)
10-IR-ZS-73[a]		56.7622	29.6650	2539	Basalt	53.52	17.6	0.1	M. Eocene (Sirjan)
10-IR-ZS-72		56.7833	29.6778	2369	Diorite	56.17	29.3	0.3	
10-IR-ZS-71[a]		56.9808	29.9225	2032	Basalt	52.16	29.0	0.2	L. Miocene (Sirjan)
10-IR-ZS-70		57.2969	29.5525	2835	Andesite	60.82	29.7	0.5	L. Eocene (Bam)
10-IR-ZS-61	Bam-Jiroft	57.6686	28.9172	1398	Gabbro	52.20	76.6	0.9	L. Jurassic (Sabzevaran)
10-IR-ZS-59[a]		57.8603	28.8375	1686	Basalt	49.44	20.5	0.2	E. Eocene (Sabzevaran)
10-IR-ZS-58		57.8664	28.8653	1665	Diorite	56.49	29.9	0.5	
10-IR-ZS-57		57.9069	29.0108	2280	Rhyolite	75.61	31.1	0.4	M. Eocene (Bam)
10-IR-ZS-55		57.9119	29.0211	2206	Green tuff	–	31.5	0.3	M. Eocene (Bam)
10-IR-ZS-56[a]		57.9119	29.0211	2206	Rhyolite	74.59	18.2	0.1	M. Eocene (Bam)
10-IR-ZS-62		57.9681	29.3158	1570	Andesite	60.02	44.9	0.5	
10-IR-ZS-53		58.3683	29.1497	1114	Andesite	64.38	38.6	0.4	
10-IR-ZS-44	Bazman	59.8639	27.7503	796	Granodiorite	67.13	72.1	0.9	
10-IR-ZS-39		60.0853	27.7325	807	Gabbro	46.59	81.1	0.9	
10-IR-ZS-40		60.0853	27.7325	807	Diorite	53.35	80.6	0.9	
10-IR-ZS-35		60.2122	27.8319	904	Granite	71.06	78.7	0.9	
d. SSZ									
09-IR-ZS-13	Hamadan	48.4439	34.7578	2187	Leucogranite	–	165.1	2.0	
09-IR-ZS-14		48.4439	34.7578	2187	Granite	68.45	163.9	1.8	
08-IR-ZS-27	Esfahan	51.9183	32.3150	1938	Granite	67.95	164.6	2.1	
10-IR-ZS-60	Jiroft	57.4339	28.7242	1384	Granite	75.18	175.2	1.8	

[a] Whole-rock Ar–Ar ages and SiO_2 contents from S.-L. Chung et al. (unpubl.)
[b] Reference ages from the 1/250,000 geological quadrangle maps of Iran (the Geological Survey of Iran) that mismatch our dating results.

the SSZ, and are plotted as histograms in Fig. A3. Most of these inherited zircons, aged from ca. 2800 to 60 Ma in the UDMA and from ca. 2500 to 220 Ma in the SSZ, were observed in certain basaltic and granitic rocks. Their age distribution in the Northwest, Central and Southeast UDMA appears peaked at ~234 Ma, ~279 Ma and ~165 Ma, respectively (Fig. A3). As mentioned above, the first two age clusters are present in two basaltic samples, i.e., 08-IR-ZS-87 (~233 Ma; Fig. 6e) and 08-IR-ZS-30 (~278 Ma; Fig. 7i), while the third is mainly from a granite sample 10-IR-ZS-35. No age peak is observed for inherited zircons from the SSZ (Fig. A3).

5. Discussion

5.1. Age distribution of magmatism in the UDMA and SSZ

The above-described age data are assembled to construct the age histograms (Fig. 10) and plotted in the sketch maps depicting the Iranian magmatic evolution through time (Fig. 11). Starting from the Middle Jurassic, four principal stages of magmatism associated with three magmatic gaps are delineated as follows:

5.1.1. The Jurassic stage

The first stage of magmatism occurred dominantly in the SSZ during the Middle and Late Jurassic (176–144 Ma), with peak activity at ~165 Ma (Fig. 10e), exposed now as intrusive bodies in the entire belt (Fig. 11a). An older "isochron" age of 199 ± 30 Ma using the whole-rock Sm–Nd method was reported from the Siah–Kuh granitoids, southwest of Kerman by Arvin et al. (2007), who argued that the subduction of the Neo-Tethys oceanic slab beneath the Iranian plate (Central Iran) may have begun since Triassic time. Mousivand et al. (2012) reported U–Pb ages of 695–181 Ma, clustering at 191 ± 12 Ma, for 33 detrital zircons from sandstones in the southeastern SSZ. These provide indirect information implying that subduction-related magmatism was probably initiated as early as the Early Jurassic, despite no such age by far has been obtained from any magmatic rocks in the SSZ.

The Jurassic Shir–Kuh pluton that exists as the oldest, and isolated, outcrop in the UDMA (Fig. 11a) needs a specific petrogenetic interpretation. Based on our unpublished geochemical results, including in-situ zircon Hf isotope data (Chiu et al., in prep.), the Shir–Kuh rocks are compositionally comparable to coeval granitoids from Hamadan and Kolah Ghazi areas in the SSZ. We hence suspect that the Shir–Kuh pluton was part of the Jurassic magmatic rocks in the SSZ, with the latter being produced by the Neotethyan subduction as generally accepted. It reached to the present configuration by more recent tectonic movements, such as strike-slip deformation along the Deh–Shir or Anar fault systems (e.g., Walker and Jackson, 2004). The tectonic deformation may have also played a role in positioning the Late Cretaceous intrusive rocks into the Southeast UDMA

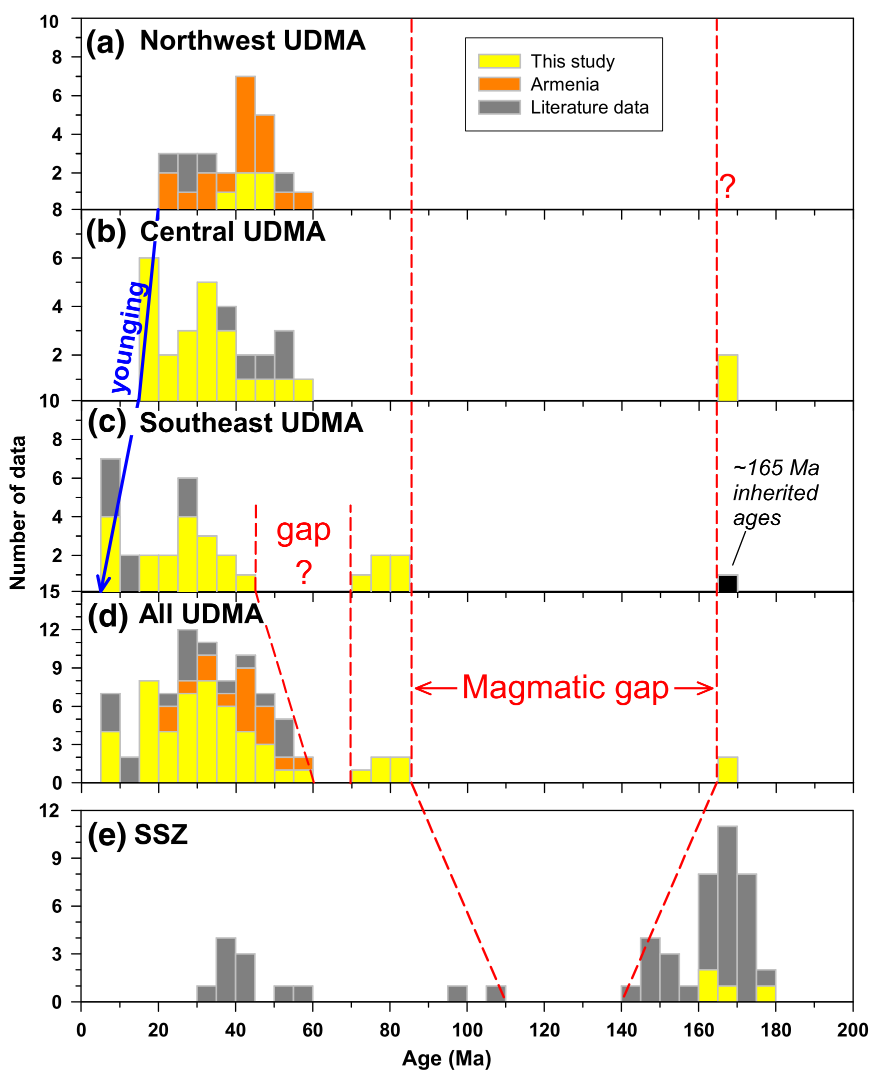

Fig. 10. Histograms of age results from (a) the Northwest UDMA, (b) the Central UDMA, (c) the Southeast UDMA, (d) all UDMA, and (e) the SSZ. Age data from Armenia are from Lin (2011) and our unpublished data.

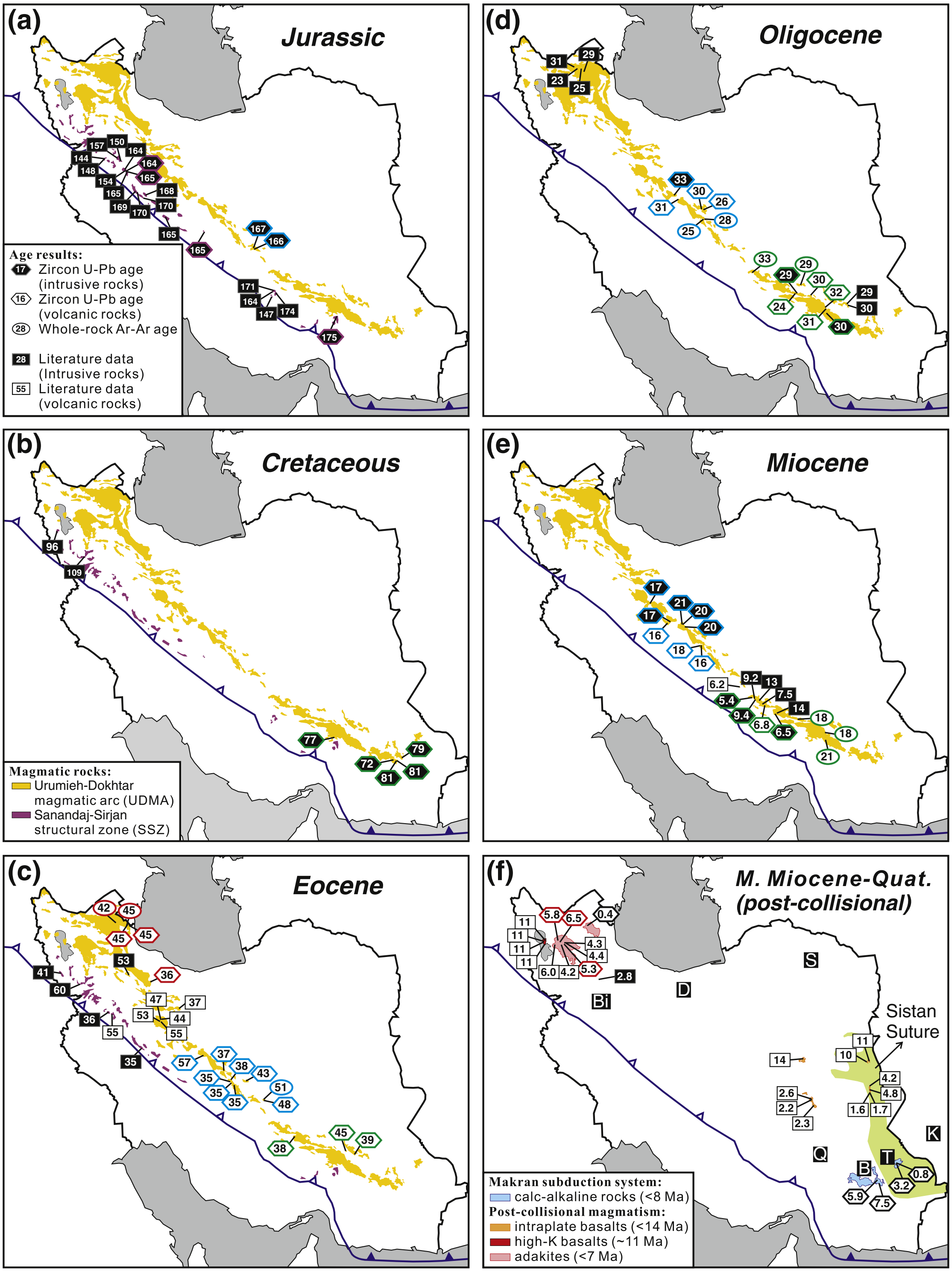

Fig. 11. Magmatic distribution in the UDMA and SSZ plotted in age spans of (a) Jurassic, (b) Late Cretaceous, (c) Eocene, (d) Oligocene, and (e) Miocene, together with (f) Middle Miocene to Quaternary post-collisional magmatism. Age data are from this study and the references listed in Table A1. In (f), unpublished ages are depicted for Bazman (ca. 8–6 Ma) and Taftan (ca. 3–1 Ma) volcanoes. B: Bazman; Bi: Bijar; D: Damavand; K: Koh-e-Sultan; Q: Qal'eh Hasan Ali Maars; S: Sar'akhor; T: Taftan.

(see next section), where four grains of Jurassic zircons (Fig. 10c) are observed in a Cretaceous granite sample.

5.1.2. The Late Cretaceous stage

Lacking igneous records in most of the Early Cretaceous (Fig. 10), the existence of the Late Cretaceous intrusive rocks in the Southeast UDMA is confirmed by this study from the Jiroft and Bazman areas (Fig. 11b). These rocks, noticeably, are exposed in the southern margin of the UDMA and approximate to the southeasternmost outcrop of the Jurassic granites (~175 Ma) in the SSZ (Fig. 11a). We reiterate the argument that young tectonic activities, in particular the shearing related to the right-lateral fault systems in southeastern Iran (Walker and Jackson, 2004), could have significantly deformed the region. Also, we note that the intrusions took place slightly later than, or broadly synchronous to, the exhumation of blueschists in the nearby Zagros and Makran areas (~105–80 Ma; Agard et al., 2006; Delaloye and Desmons, 1980), suggesting a change in the convergence rate between Arabia and Eurasia (Agard et al., 2006) that may have changed the Neotethyan subduction framework and thus accounted for the renewal of arc magmatism at this specific period of time.

In addition to the two zircon U–Pb ages of 109 and 96 Ma listed in Table A1 and plotted in Fig. 11b, Cretaceous ages between 136 and 65 Ma have been documented for some granitoid complexes in the northwestern SSZ by using conventional K–Ar and Rb–Sr dating methods (e.g., Baharifar et al., 2004; Braud and Bellon, 1974; Ghalamghash et al., 2009; Masoudi et al., 2002; Valizadeh and Cantagrel, 1975). These K-Ar and Rb–Sr data, however, may better be interpreted as indicating ages of later metamorphic events, rather than those of magmatic emplacements, in this part of the SSZ. Their geologic meaning awaits more detailed dating analyses to validate.

5.1.3. The Eocene–Oligocene stage

After a short (~15 m.y.) magmatic gap, from ca. 72 to 57 Ma (Fig. 10d), magmatism in the UDMA was most active and widespread in the Eocene and Oligocene, ca. 55–25 Ma, during this ~30 m.y. time period igneous rocks typical of calc-alkaline geochemistry are identified in the entire magmatic belt (Fig. 11; c and d). Such a prolonged, and steady, igneous "flare-up" activity over the UDMA has never been envisioned by previous workers (e.g., Alavi, 1994; Berberian and King, 1981; Omrani et al., 2008; Verdel et al., 2011) that generally thought the UDMA to have been overwhelmed by a major volcanic pulse in the Eocene with limited activities in the Oligocene (cf. Agard et al., 2011; for review). Omrani et al. (2008), more specifically, argued a magmatic quiescence in the UDMA from the Oligocene to Early Miocene and proposed that Arabia started colliding with Eurasia at this time. The Iranian literature is full of publications that, as shown in the geological maps, suggests the volcanic nature of an Eocene peak and the scarcity of Oligocene volcanic successions (cf. Allen and Armstrong, 2008; for summary), however, we address that our new age data do not support such an argument. This urges the necessity of carefully reevaluating the age distribution of Cenozoic volcanic and associated sedimentary sequences by further detailed studies in Iran. Furthermore, we emphasize that the data from Armenia show a similar magmatic duration from ca. 57 to 22 Ma (Fig. 10a), reinforcing the notion that calc-alkaline rocks also lasting from the Eocene to Oligocene in Armenia represent the arc product as a continuation of the northwest UDMA (Lin, 2011; Lin et al., 2011).

A total of 10 Paleogene ages from ca. 60 to 35 Ma (Table A1) are now available from the northwestern part of the SSZ in five localities, in contrast to the southeastern SSZ where Cenozoic igneous rocks appear not existing (Fig. 11c). This seems to support the view of dividing the SSZ into two parts (Eftekharnejad, 1981; Ghasemi and Talbot, 2006): (1) the South SSZ that consists essentially of rocks deformed and/or metamorphosed in the Triassic and Jurassic; and (2) the North SSZ that was deformed in the Late Cretaceous and intruded by felsic rocks in the localities in the Cenozoic.

5.1.4. The Miocene stage

Magmatism ceased at ~23 Ma in the Northwest UDMA but was still active in the Central and Southeast UDMA (Fig. 11e), where our data indicate magmatic activity lasting from ca. 21 to 6 Ma and ending with small-volume intrusions. We note here that many rocks of the ending phases, ~27–22 Ma, ~17–16 Ma and ~10–6 Ma in Armenia, and Central and Southeast UDMA, respectively, are characterized by adakitic geochemical affinities (Chung et al., unpubl. data). In Section 5.2.3, a more detailed discussion on this regard will be given. Some workers (e.g., Omrani et al., 2008; Shafiei et al., 2009) have argued, without precise age constraints, that adakitic rocks occur in the Central and Southeast UDMA from the Middle Miocene to Pliocene–Quaternary as post-collisional magmatic products. We do not agree with such an argument and will cast relevant discussion in the latter section.

The "real" post-collisional magmatism in the UDMA, i.e., magmatism postdating Arabia started colliding with Eurasia, began in the northwest part at ~11 Ma (Fig. 11f), occurring as high-K basalts in Saray located just east off the Urumieh Lake (Fig. 2). These high-K rocks, termed as absarokite (Chiu et al., 2010) or more specifically plagioleucitite (Pang et al., in review), erupting after an ~10 m.y. magmatic gap (Fig. 12), represent a compositionally unique component and one of the earliest phases of the vast post-collisional volcanic field that covers much of the Lesser Caucasus, NW Iran and eastern Anatolia regions (Dilek et al., 2010; Keskin, 2003; Kheirkhah et al., 2009; Lin, 2011; Lin et al., 2011; Pearce et al., 1990). In the Alpine–Himalayan orogenic belt, such as in Tibet (Chung et al., 2005) and western Anatolia (Aldanmaz et al., 2000), the occurrence of potassic to ultrapotassic rocks has been generally regarded as a marker for the onset of post-collisional magmatism. More discussions on the post-collisional magmatism in Iran will be texted in Section 5.2.4.

5.2. Further implications from UDMA records

5.2.1. Inland migration of arc magmatism after a long quiescence

The SSZ has long been considered as an Andean-type margin marked with calc-alkaline magmatic activity that was most active in the early Mesozoic and migrated northward in the later half of the Mesozoic (e.g., Agard et al., 2005, 2011; Berberian and King, 1981; Stöcklin, 1968). This study indicates that the northward, or inland, migration may have associated with a long magmatic gap or quiescence time (Fig. 10), given the observation that arc magmatism renewed in the UDMA at ~80 Ma and became widespread since the Early Eocene. A simple, and perhaps thus popular, interpretation for this migration is the change in the Neotethyan subduction angle (e.g., Agard et al., 2011; Berberian and Berberian, 1981; Shahabpour, 2007), such that described by Verdel et al. (2011) who suggested that the flattening of the subduction have shifted the arc magmatism from the SSZ in the Mesozoic to the UDMA in the Tertiary.

5.2.2. Eocene–Oligocene magmatic flare-ups in Iran

Our age data suggest that the UDMA volcanism was most active and widespread during the Eocene and Oligocene (ca. 55–25 Ma),

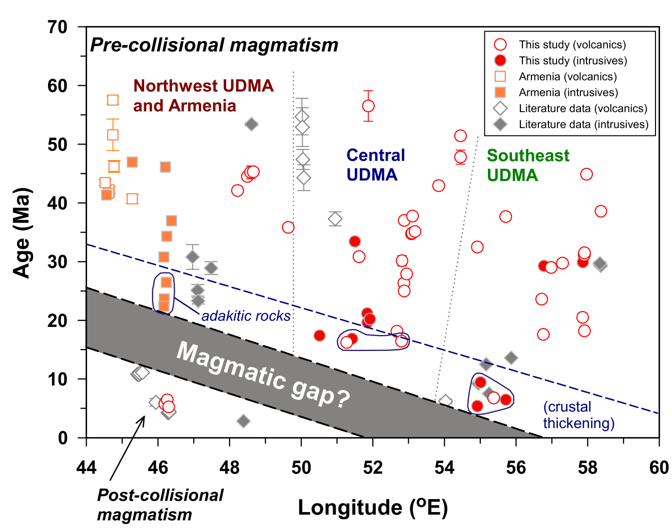

Fig. 12. Age versus space plot of dated samples from the UDMA and Armenia. Note that in NW Iran the "pre-collisional" arc magmatism ceased at ~22 Ma and "post-collisional" magmatism started at ~11 Ma, with a magmatic gap of ~10 m.y. Note that the occurrence of adakitic rocks in the ending phase of arc magmatism suggests crustal thickening caused by the initial collision. See text for discussion.

much longer lasting than previously thought as just an Eocene pulse. This would require a protracted, and steady, subduction system that must have started operating since the Early Eocene. Such a scenario of prolonged magmatic flare-ups, moreover, may have existed also in other parts of Iran, such as the Alborz Range, Central Iran and Lut block (Fig. 1c), where Eocene igneous rocks are extensive and well documented (Axen et al., 2001; Horton et al., 2008; Karimpour et al., 2011b; Malekzadeh et al., 2010; Ramezani and Tucker, 2003; Verdel et al., 2007, 2011). For example, our ongoing study in the northern Sistan and Lut regions suggests the presence of widespread calc-alkaline volcanism during ca. 45 to 25 Ma that may be interpreted by an extensional tectonic environment postdating the suturing between the Lut and Afghan blocks (Pang et al., 2011, 2012; Zarrinkoub et al., 2010, 2012). Furthermore detailed investigations regarding magmatism of this stage in the Alborz and Central Iran are needed so that a comprehensive understanding of the magmatic and tectonic evolution from the Eocene to Oligocene in the entire country may be achieved.

5.2.3. Southeastward cessation of UDMA magmatism

As a whole, the UDMA appears to have been a magmatic arc that lasted steadily or at least semi-continuously from ca. 55 to 6 Ma (Fig. 10d). Cessation of the arc magmatism, however, took place progressively from the northwest to the southeast (Fig. 12), i.e., ending at ~22 Ma in the Early Miocene in the Meghri complex, southeastern Armenia (Fig. 2), ~16 Ma in the Middle Miocene in the Kashan area (Fig. 3), and ~9–6 Ma in the Late Miocene in the Anar area (Fig. 4). This southeastward termination of the UDMA magmatism is consistent with the notion of oblique and thus diachronous collision between Arabia and Eurasia, with the collision initiating in the northwest and propagating progressively to the southeast along the Zagros suture zone. All these may have been accompanied with counterclockwise rotation of the Arabian block, as evidenced by the modern GPS data (ArRajehi et al., 2010; Vernant et al., 2004).

There are associated changes in the geochemical compositions of the UDMA rocks (Chung et al., unpubl. data). Granitoids from the Meghri complex, lasting from ca. 46–22 Ma, show a significant geochemical variation from I-type calc-alkaline (≥30 Ma) to adakitic (27–22 Ma) characteristics (Fig. 12) that we attribute to collision-resultant thickening of the arc crust in the region. Similar features, i.e., transition from calc-alkaline to adakitic magmatism, are observed southeastward, with adakitic rocks occurring as the ending phases in the Central (ca. 17–16 Ma) and Southeast (ca.10–6 Ma) UDMA, which we interpret to be a consequence of the southeastward crustal thickening owing to the diachronous collision (Fig. 12). It is beyond the scope of this paper to get into further detail, which will be discussed in a separate article in preparation. We just address that analogous examples have been reported in southern Tibet where the final stage of the Gangdese arc magmatism lasted semi-continuously from ca. 65 to 34 Ma and the emplacement of adakitic granitoids indicative of collision-related crustal thickening began since ~51 Ma (cf. Ji et al., 2012). Under this framework of comparison, we infer that the collision between Arabia and Eurasia appears to have started no later than ca. 30 Ma when the Meghri granitoids began showing adakitic geochemical signatures. Then, the collision propagated southeastward and Arabia should have started colliding with Eurasia in the southeastern part by ca. 10 Ma, when the UDMA magmatism there started changing the geochemical composition from calc-alkaline to adakitic affinities (Fig. 12). In other words, we argue that the collision started diachronously in the northwest and southeast before ~30 Ma and ~10 Ma, respectively, thus causing crustal thickening that led to magma's compositional change from calc-alkaline to adakitic. This ending phase of magmatism, however, did not cease at once but lasted for several more million years until ~22 and ~6 Ma, respectively.

5.2.4. Post-collisional volcanism in Iran

The Arabia–Eurasia collision resulted in the unusual occurrence of a voluminous volcanic field that erupted from the Caucasus to eastern Anatolia and NW Iran starting ca. 15–11 Ma (Keskin, 2003; Keskin et al., 2010; Lebedev et al., 2010; Pearce et al., 1990; and references therein). It is noted that the earliest eruption, aging 15.0–13.5 Ma based on K–Ar dating data, occurs in the Alada complex, the northern Van neovolcanic province (Lebedev et al., 2010). This study, and our unpublished results from Georgia and Armenia, identifies the occurrence of several specific magma types including (1) the Middle Miocene (~11 Ma) high-K basalts from Saray, NW Iran, and (2) extensive adakites that occurred not only in Sahand (ca. 6–4 Ma) and Sabalan (~0.4 Ma), NW Iran, but also in central Armenia (~4 Ma), southern Georgia (~3 Ma) and even as north to Kazbegi, the Greater Caucasus (<1 Ma). Here we note that the scenario of the associated occurrence of high-K and adakitic magmas in the post-collisional setting, NW Iran (Figs. 11f and 12) is analogous to what have been observed in southern Tibet (cf. Chung et al., 2005), where associated ultrapotassic and adakitic rocks are generally interpreted as products from melting the metasomatized lithospheric mantle and the eclogitized lower crust, respectively, related to lithospheric thickening and subsequent delamination.

From the Middle Miocene, additional types of volcanism took place in southeastern Iran (Fig. 11f). In the Sistan suture zone and Lut block, intraplate alkali basalts erupted from ~14 Ma to the Quaternary under a "post-collisional" extension regime that has been proposed as a result of suturing between the Lut and Afghan blocks (Pang et al., 2012; Walker et al., 2009). This extension regime may have been affiliated and/or interacted with the active Makran subduction in the south that has produced three arc volcanoes, namely, Bazman and Taftan in Iran and Koh-e-Sultan in Pakistan (Biabangard and Moradian, 2008; Saadat and Stern, 2011). Our unpublished data (Fig. 11f) suggest that eruptions in the Bazman and Taftan volcanoes occurred in the Late Miocene (ca. 8–6 Ma) and Late Pliocene to Quaternary (ca. 3–1 Ma), respectively. In addition, there are at least four "isolated" young volcanic fields having been documented (Fig. 11f): (1) Mt. Damavand that consists mainly of shoshonites erupting since ~2 Ma (Davidson et al., 2004); (2) Mt. Sar'akhor that consists of dacitic lavas dated at ~2–3 Ma (Shabanian et al., 2009); (3) the Qal'eh Hasan Ali Maars that erupted in the Southeast UDMA and consists of Quaternary tephrites (Milton, 1977); and (4) the Bijar volcanic area that consists of Late Miocene high-K calc-alkaline and Pleistocene potassic alkaline rocks (Boccaletti et al., 1976). All these young eruptions warrant detailed investigations for their petrogenesis and regional tectonic significance.

Acknowledgements

We thank H. Azizi and K.-N. Pang for their help in the fieldwork and C.-H. Hung for the assistance with the LA-ICPMS experiment, and two anonymous journal reviewers for their thoughtful and constructive comments that helped improve the paper. This study was performed under a joint research program supported by the National Taiwan University and the Birjand University; and the NTU team was supported by research grants from the National Science Council, Taiwan, ROC to SLC, in particular the grant NSC100-2745-M-002-001-ASP.

Appendix A. Supplementary data

Supplementary data to this article can be found online at http://dx.doi.org/10.1016/j.lithos.2013.01.006.

References

Agard, P., Omrani, J., Jolivet, L., Mouthereau, F., 2005. Convergence history across Zagros (Iran): constraints from collisional and earlier deformation. International Journal of Earth Sciences 94, 401–419.

Agard, P., Monie, P., Gerber, W., Omrani, J., Molinaro, M., Meyer, B., Labrousse, L., Vrielynck, B., Jolivet, L., Yamato, P., 2006. Transient, synobduction exhumation of Zagros blueschists inferred from P–T, deformation, time, and kinematic constraints: implications for Neotethyan wedge dynamics. Journal of Geophysical Research 111, B11401 http://dx.doi.org/10.1029/2005JB004103.

Agard, P., Omrani, J., Jolivet, L., Whitechurch, H., Vrielynck, B., Spakman, W., Monié, P., Meyer, B., Wortel, R., 2011. Zagros orogeny: a subduction-dominated process. Geological Magazine 148, 692–725.

Aghazadeh, M., Castro, A., Omran, N.R., Emami, M.H., Moinvaziri, H., Badrzadeh, Z., 2010. The gabbro (shoshonitic)–monzonite–granodiorite association of Khankandi pluton, Alborz Mountains, NW Iran. Journal of Asian Earth Sciences 38, 199–219.

Aghazadeh, M., Castro, A., Badrzadeh, Z., Vogt, K., 2011. Post-collisional polycyclic plutonism from the Zagros hinterland: the Shaivar Dagh plutonic complex, Alborz belt, Iran. Geological Magazine 148, 980–1008.

Ahmadi Khalaji, A., Esmaeily, D., Valizadeh, M.V., Rahimpour-Bonab, H., 2007. Petrology and geochemistry of the granitoid complex of Boroujerd, Sanandaj–Sirjan Zone, Western Iran. Journal of Asian Earth Sciences 29, 859–877.

Alavi, M., 1980. Tectonostratigraphic evolution of the Zagrosides of Iran. Geology 8, 144–149.

Alavi, M., 1994. Tectonics of the Zagros orogenic belt of Iran: new data and interpretations. Tectonophysics 229, 211–238.

Alavi, M., 2004. Regional stratigraphy of the Zagros fold–thrust belt of Iran and its proforeland evolution. American Journal of Science 304, 1–20.

Alavi, M., 2007. Structures of the Zagros fold–thrust belt in Iran. American Journal of Science 307, 1064–1095.

Aldanmaz, E., Pearce, J., Thirlwall, M., Mitchell, J., 2000. Petrogenetic evolution of late Cenozoic, post-collision volcanism in western Anatolia, Turkey. Journal of Volcanology and Geothermal Research 102, 67–95.

Alirezaei, S., Hassanzadeh, J., 2012. Geochemistry and zircon geochronology of the Permian A-type Hasanrobat granite, Sanandaj-Sirjan belt: A new record of the Gondwana breal-up in Iran. Lithos 151, 122–134.

Allen, M.B., Armstrong, H.A., 2008. Arabia–Eurasia collision and the forcing of mid-Cenozoic global cooling. Palaeogeography, Palaeoclimatology, Palaeoecology 265, 52–58.

Allen, M.B., Mark, D.F., Kheirkhah, M., Barfod, D., Emami, M.H., Saville, C., 2011. $^{40}Ar/^{39}Ar$ dating of Quaternary lavas in northwest Iran: constraints on the landscape evolution and incision rates of the Turkish–Iranian plateau. Geophysical Journal International 185, 1175–1188.

Anderson, T., 2002. Correction of common lead in U–Pb analyses that do not report ^{204}Pb. Chemical Geology 192, 59–79.

ArRajehi, A., McClusky, S., Reilinger, R., Daoud, M., Alchalbi, A., Ergintav, S., Gomez, F., Sholan, J., Bou-Rabee, F., Ogubazghi, G., Haileab, B., Fisseha, S., Asfaw, L., Mahmoud, S., Rayan, A., Bendik, R., Kogan, L., 2010. Geodetic constraints on present-day motion of the Arabian Plate: implications for Red Sea and Gulf of Aden rifting. Tectonics 29, TC3011 http://dx.doi.org/10.1029/2009TC002482.

Arvin, M., Pan, Y., Dargahi, S., Malekizadeh, A., Babaei, A., 2007. Petrochemistry of the Siah-Kuh granitoid stock southwest of Kerman, Iran: implications for initiation of Neotethys subduction. Journal of Asian Earth Sciences 30, 474–489.

Axen, G.J., Lam, P.S., Grove, M., Stockli, D.F., Hassanzadeh, J., 2001. Exhumation of the west-central Alborz Mountains, Iran, Caspian subsidence, and collision-related tectonics. Geology 29, 559–562.

Azizi, H., Moinevaziri, H., 2009. Review of the tectonic setting of Cretaceous to Quaternary volcanism in northwestern Iran. Journal of Geodynamics 47, 167–179.

Azizi, H., Chung, S.-L., Tanaka, T., Asahara, Y., 2011a. Isotopic dating of the Khoy metamorphic complex (KMC), northwestern Iran: a significant revision of the formation age and magma source. Precambrian Research 185, 87–94.

Azizi, H., Asahara, Y., Mehrabi, B., Chung, S.-L., 2011b. Geochronological and geochemical constraints on the petrogenesis of high-K granite from the Suffi abad area, Sanandaj–Sirjan zone, NW Iran. Chemie der Erde 71, 363–376.

Azizi, H., Tanaka, T., Asahara, Y., Chung, S.-L., Zarrinkoub, M.H., 2011c. Discrimination of the age and tectonic setting for magmatic rocks along the Zagros thrust zone, northwest Iran, using the zircon U–Pb age and Sr–Nd isotopes. Journal of Geodynamics 52, 304–320.

Bagheri, S., Stampfli, G.M., 2008. The Anarak, Jandaq and Posht-e-Badam metamorphic complexes in central Iran: new geological data, relationships and tectonic implications. Tectonophysics 451, 123–155.

Baharifar, A., Moinevaziri, H., Bellon, H., Piqué, A., 2004. The crystalline complexes of Hamadan (Sanandaj–Sirjan zone, western Iran): metasedimentary Mesozoic sequences affected by Late Cretaceous tectono-metamorphic and plutonic events. Comptes Rendus Geosciences 336, 1443–1452.

Ballato, P., Uba, C.E., Landgraf, A., Strecker, M.R., Sudo, M., Stockli, D.F., Friedrich, A., Tabatabaei, S.H., 2011. Arabia–Eurasia continental collision: insights from late Tertiary foreland-basin evolution in the Alborz Mountains, northern Iran. Geological Society of America Bulletin 123, 106–131.

Bea, F., Mazhari, A., Montero, P., Amini, S., Ghalamghash, J., 2011. Zircon dating, Sr and Nd isotopes, and element geochemistry of the Khalifan pluton, NW Iran: evidence for Variscan magmatism in a supposedly Cimmerian superterrane. Journal of Asian Earth Sciences 40, 172–179.

Berberian, F., Berberian, M., 1981. Tectono-plutonic episodes in Iran. In: Gupta, H.K., Delany, F.M. (Eds.), Zagros–Hindu Kush–Himalaya Geodynamic Evolution: American Geophysical Union, Geodynamics Series, 3, pp. 5–32.

Berberian, M., King, G.C.P., 1981. Towards a paleogeography and tectonic evolution of Iran. Canadian Journal of Earth Sciences 18, 210–265.

Berberian, F., Muir, I.D., Pankhurst, R.J., Berberian, M., 1982. Late Cretaceous and early Miocene Andean-type plutonic activity in northern Makran and Central Iran. Journal of the Geological Society of London 139, 605–614.

Biabangard, H., Moradian, A., 2008. Geology and geochemical evaluation of Taftan Volcano, Sistan and Baluchestan Province, southeast of Iran. Chinese Journal of Geochemistry 27, 356–369.

Boccaletti, M., Innocenti, F., Manetti, P., Mazzuoli, R., Motamed, A., Pasquaré, G., Radicati di Brozolo, F., Amin Sobhani, E., 1976. Neogene and Quaternary volcanism of the Bijar area (western Iran). Bulletin of Volcanology 40, 121–132.

Braud, J., Bellon, H., 1974. Données nouvelles sur le domaine métamorphique du Zagros (zone de Sanandaj–Sirjan) au niveau de Kermanshah–Hamadan (Iran): nature âge et interprétation des séries métamorphiques et des intrusions; évolution structurale. Rapport Université Paris-Sud, pp. 1–20.

Chiu, H.-Y., Chung, S.-L., Wu, F.-Y., Liu, D., Liang, Y.-H., Lin, I.-J., Iizuka, Y., Xie, L.-W., Wang, Y., Chu, M.-F., 2009. Zircon U-Pb and Hf isotopic constraints from eastern Transhimalayan batholiths on the precollisional magmatic and tectonic evolution in southern Tibet. Tectonophysics 477, 3–19.

Chiu, H.-Y., Zarrinkoub, M.H., Chung, S.-L., Lin, I.-J., Yang, H.-H., Lo, C.-H., Mohammadi, S.S., Khatib, M.M., 2010. Zircon U–Pb age and geochemical constraints on the magmatic and tectonic evolution in Iran. In: Dilek, Y., et al. (Ed.), Tectonic Crossroads: Evolving Orogens of Eurasia–Africa–Arabia, Ankara, Turkey: Geol. Soc. Amer. Abstract Volume, p. 31.

Chung, S.L., Chu, M.F., Zhang, Y., Xie, Y., Lo, C.H., Lee, T.Y., Lan, C.Y., Li, X., Zhang, Q., Wang, Y., 2005. Tibetan tectonic evolution inferred from spatial and temporal variations in post-collisional magmatism. Earth-Science Reviews 68, 173–196.

Dargahi, S., Arvin, M., Pan, Y., Babaei, A., 2010. Petrogenesis of post-collisional A-type granitoids from the Urumieh–Dokhtar magmatic assemblage, Southwestern Kerman, Iran: constraints on the Arabian–Eurasian continental collision. Lithos 115, 190–204.

Davidson, J., Hassanzadeh, J., Berzins, R., Stockli, D.F., Bashukooh, B., Turrin, B., Pandamouz, A., 2004. The geology of Damavand volcano, Alborz Mountains, northern Iran. Geological Society of America Bulletin 116, 16–29.

Delaloye, M., Desmons, J., 1980. Ophiolites and mélange terranes in Iran: a geochronological study and its paleotectonic implications. Tectonophysics 68, 83–111.

Dilek, Y., Imamverdiyev, N., Altunkaynak, Ş., 2010. Geochemistry and tectonics of Cenozoic volcanism in the Lesser Caucasus (Azerbaijan) and the peri-Arabian region: collision-induced mantle dynamics and its magmatic fingerprint. International Geology Review 52, 536–578.

Eftekharnejad, J., 1981. Tectonic division of Iran with respect to sedimentary basins. Journal of Iranian Petroleum Society 83, 19–28 (in Persian).

Emami, M.H., 1981. Geological quadrangle map of Iran, 1:250,000 scale, sheet E6 (Qom), the Geological Survey of Iran.

Esna-Ashari, A., Tiepolo, M., Valizadeh, M.V., Hassanzadeh, J., Sepahi, A.A., 2012. Geochemistry and zircon U-Pb geochronology of Aligoodarz granitoid complex, Sanandaj-Sirjan zone, Iran. Journal of Asian Earth Sciences 43, 11–22.

Fazlnia, A., Moradian, A., Rezaei, K., Moazzen, M., Alipour, S., 2007. Synchronous activity of anorthositic and S-type granitic magmas in Chah–Dozdan Batholith, Neyriz, Iran: evidence of zircon SHRIMP and monazite CHIME dating. Journal of Sciences, Islamic Republic of Iran 18, 221–237.

Fazlnia, A., Schenk, V., van der Straaten, F., Mirmohammadi, M., 2009. Petrology, geochemistry, and geochronology of trondhjemites from the Qori Complex, Neyriz, Iran. Lithos 112, 413–433.

Ghalamghash, J., Nédélec, A., Bellon, H., Vousoughi Abedini, M., Bouchez, J.L., 2009. The Urumieh plutonic complex (NW Iran): a record of the geodynamic evolution of the Sanandaj–Sirjan zone during Cretaceous times — part I: petrogenesis and K/Ar dating. Journal of Asian Earth Sciences 35, 401–415.

Ghasemi, A., Talbot, C.J., 2006. A new tectonic scenario from the Sanandaj–Sirjan Zone (Iran). Journal of Asian Earth Sciences 26, 683–693.

Ghavidel-Syooki, M., Hassanzadeh, J., Vecoli, M., 2011. Palynology and isotope geochronology of the Upper Ordovician–Silurian successions (Ghelli and Soltan Maidan Formations) in the Khoshyeilagh area, eastern Alborz Range, northern Iran; stratigraphic and palaeogeographic implications. Review of Palaeobotany and Palynology 164, 251–271.

Guest, B., Stockli, D.F., Grove, M., Axen, G.J., Lam, P.S., 2006. Thermal histories from the central Alborz Mountains, northern Iran: implications for the spatial and temporal distribution of deformation in northern Iran. Geological Society of America Bulletin 118, 1507–1521.

Hassanzadeh, J., Stockli, D.F., Horton, B.K., Axen, G.J., Stockli, L.D., Grove, M., Schmitt, A.K., Walker, J.D., 2008. U–Pb zircon geochronology of late Neoproterozoic–Early Cambrian granitoids in Iran: implications for paleogeography, magmatism, and exhumation history of Iranian basement. Tectonophysics 451, 71–96.

Horton, B.K., Hassanzadeh, J., Stockli, D.F., Axen, G.J., Gillis, R.J., Guest, B., Amini, A., Fakhari, M.D., Zamanzadeh, S.M., Grove, M., 2008. Detrital zircon provenance of Neoproterozoic to Cenozoic deposits in Iran: implications for chronostratigraphy and collisional tectonics. Tectonophysics 451, 97–122.

Hoskin, P.W.O., Schaltegger, U., 2003. The composition of zircon and igneous and metamorphic petrogenesis. In: Manchar, J.M., Hoskin, P.W.O. (Eds.), Zircon: Reviews of Mineralogy and Geochemistry, 53, pp. 27–62.

Hosseini, Z., Ghaemi, J., Mohabbi, A.R., 1995. Geological quadrangle map of Iran, 1:250,000 scale, sheet I11 (Sirjan), the Geological Survey of Iran.

Ireland, T.R., Williams, I.S., 2003. Considerations in zircon geochronology by SIMS. In: Manchar, J.M., Hoskin, P.W.O. (Eds.), Zircon: Reviews of Mineralogy and Geochemistry, 53, pp. 215–241.

Jackson, S.E., Pearson, N.J., Griffin, W.L., Belousova, E.A., 2004. The application of laser ablation-inductively coupled plasma-mass spectrometry to in situ U–Pb zircon geochronology. Chemical Geology 211, 47–69.

Ji, W.-Q., Wu, F.-Y., Liu, C.-Z., Chung, S.-L., 2012. Early Eocene crustal thickening in southern Tibet: new age and geochemical constraints from the Gangdese batholith. Journal of Asian Earth Sciences 53, 82–95.

Karimpour, M.H., Stern, C.R., Farmer, G.L., 2010. Zircon U–Pb geochronology, Sr–Nd isotope analyses, and petrogenetic study of the Dehnow diorite and Kuhsangi granodiorite (Paleo-Tethys), NE Iran. Journal of Asian Earth Sciences 37, 384–393.
Karimpour, M.H., Farmer, G.L., Stern, C.R., Salati, E., 2011a. U–Pb zircon geochronology and Sr–Nd isotopic characteristic of Late Neoproterozoic Bornaward granitoids (Taknar zone exotic block), Iran. Iranian Journal of Crystallography and Mineralogy 19, 1–18.
Karimpour, M.H., Stern, C.R., Farmer, L., Saadat, S., Malekezadeh, A., 2011b. Review of age, Rb–Sr geochemistry and petrogenesis of Jurassic to Quaternary igneous rocks in Lut Block, Eastern Iran. Geopersia 1, 19–36.
Keskin, M., 2003. Magma generation by slab steepening and breakoff beneath a subduction–accretion complex: an alternative model for collision-related volcanism in Eastern Anatolia, Turkey. Geophysical Research Letters 30 (24), 8046 http://dx.doi.org/10.1029/2003GL018019.
Keskin, M., Lebedev, V., Sharkov, E., Oyan, V., Unal, E., 2010. A new look at the collision-related volcanism in Eastern Anatolia, Turkey: volcanic history of the northern Van neovolcanic province. Geophysical Research Abstracts 12 (EGU2010-12629).
Kheirkhah, M., Allen, M., Emami, M., 2009. Quaternary syn-collision magmatism from the Iran–Turkey borderlands. Journal of Volcanology and Geothermal Research 182, 1–12.
Kouhestani, H., Ghaderi, M., Zaw, K., Meffre, S., Emami, M.H., 2012. Geological setting and timing of the Chah Zard breccia-hosted epithermal gold–silver deposit in the Tethyan belt of Iran. Mineralium Deposita 47, 425–440.
Lebedev, V.A., Sharkov, E.V., Keskin, M., Oyan, V., 2010. Geochronology of late Cenozoic volcanism in the area of Lake Van, Turkey: an example of developmental dynamics for magmatic processes. Doklady Earth Sciences 433, 1031–1037.
Li, X.-H., Liu, Y., Li, Q.-L., Guo, C.-H., Chamberlain, K.R., 2009. Precise determination of Phanerozoic zircon Pb/Pb age by multicollector SIMS without external standardization. Geochemistry, Geophysics, Geosystems 10 (4), Q04010 http://dx.doi.org/10.1029/2009GC002400.
Lin, Y.-C., 2011. Geochemical characteristics and petrogenesis of pre- to post-collisional igneous rocks in Armenia and Caucasian regions. MSc Thesis, National Taiwan University (in Chinese with English abstract).
Lin, Y.-C., Chung, S.-L., Karakhanyan, A., Jrbashyan, R., Navasardyan, G., Galoyan, G., Chiu, H.-Y., Lin, I.-J., Chu, C.-H., Lee, H.-Y., 2011. Geochemical and Sr–Nd isotopic constraints on the petrogenesis of pre- to post-collisional volcanic rocks in Armenia. EGU General Assembly 2011. Geophysical Research Abstracts 13 (EGU2011-5422).
Ludwig, K.R., 2003. Isoplot v. 3.0: a geochronological toolkit for Microsoft Excel. Berkeley Geochronology Center, Special Publication No. 4 (70 pp.).
Mahmoudi, S., Masoudi, F., Corfu, F., Mehrabi, B., 2010. Magmatic and metamorphic history of the Deh–Salm metamorphic Complex, Eastern Lut block, (Eastern Iran), from U–Pb geochronology. International Journal of Earth Sciences 99, 1153–1165.
Mahmoudi, S., Corfu, F., Masoudi, F., Mehrabi, B., Mohajjel, M., 2011. U–Pb dating and emplacement history of granitoid plutons in the northern Sanandaj–Sirjan Zone, Iran. Journal of Asian Earth Sciences 41, 238–249.
Malekzadeh, A., Karimpour, M.H., Mazaheri, S.A., 2010. Rb–Sr and Sm–Nd isotopic compositions and petrogenesis of ore-related intrusive rocks of gold-rich porphyry copper Maherabad prospect area (North of Hanich), east of Iran. Iranian Journal of Crystallography and Mineralogy 18, 15–32.
Masoudi, F., Yardley, B.W.D., Cliff, R.A., 2002. Rb–Sr geochronology of pegmatites, plutonic rocks and a hornfels in the region south-west of Arak, Iran. Journal of Sciences, Islamic Republic of Iran 13, 249–254.
Mazhari, S.A., Bea, F., Amini, S., Ghalamghash, J., Molina, J.F., Montero, P., Scarrow, J.H., Williams, I.S., 2009. The Eocene bimodal Piranshahr massif of the Sanandaj–Sirjan Zone, NW Iran: a marker of the end of the collision in the Zagros orogen. Journal of the Geological Society of London 166, 53–69.
Mazhari, S.A., Amini, S., Ghalamghash, J., Bea, F., 2011. Petrogenesis of granitic unit of Naqadeh complex, Sanandaj–Sirjan Zone, NW Iran. Arabian Journal of Geosciences 4, 59–67.
McInnes, B.I.A., Evans, N.J., Belousova, E., Griffin, W.L., 2003. Porphyry copper deposits of the Kerman belt, Iran: timing of mineralization and exhumation processes. CSIRO Scientific Research Report, 41.
McInnes, B.I.A., Evans, N.J., Fu, F.Q., Garwin, S., 2005. Application of thermochronology to hydrothermal ore deposits. Reviews in Mineralogy and Geochemistry 58, 467–498.
McQuarrie, N., Stock, J.M., Verdel, C., Wernicke, B.P., 2003. Cenozoic evolution of Neotethys and implications for the causes of plate motions. Geophysical Research Letters 30 (20), 2036 http://dx.doi.org/10.1029/2003GL017992.
Milton, D.J., 1977. Qal'eh Hasan Ali Marrs, central Iran. Bulletin of Volcanology 40, 201–208.
Moghadam, H.S., Stern, R.J., Rahgoshay, M., 2010. The Dehshir ophiolite (central Iran): geochemical constraints on the origin and evolution of the Inner Zagros ophiolite belt. Geological Society of America Bulletin 122, 1516–1547.
Mohajjel, M., Fergusson, C.L., 2000. Dextral transpression in Late Cretaceous continental collision, Sanandaj–Sirjan zone, Western Iran. Journal of Structural Geology 22, 1125–1139.
Mohajjel, M., Fergusson, C.L., Sahandi, M.R., 2003. Cretaceous–Tertiary convergence and continental collision, Sanandaj–Sirjan Zone, western Iran. Journal of Asian Earth Sciences 21, 397–412.
Mousivand, F., Rastad, E., Meffre, S., Peter, J.M., Solomon, M., Zaw, K., 2011. U–Pb geochronology and Pb isotope characteristics of the Chahgaz volcanogenic massive sulphide deposit, southern Iran. International Geology Review 53, 1239–1262.
Mousivand, F., Rastad, E., Meffre, S., Peter, J.M., Mohajjel, M., Zaw, K., Emami, M.H., 2012. Age and tectonic setting of the Bavanat Cu–Zn–Ag Besshi-type volcanogenic massive sulfide deposit, southern Iran. Mineralium Deposita http://dx.doi.org/10.1007/s00126-012-0407-6.
Okay, A.I., Zattin, M., Cavazza, W., 2010. Apatite fission-track data for the Miocene Arabia–Eurasia collision. Geology 38, 35–38.
Omrani, J., Agard, P., Whitechurch, H., Benoit, M., Prouteau, G., Jolivet, L., 2008. Arc-magmatism and subduction history beneath the Zagros Mountains, Iran: a new report of adakites and geodynamic consequences. Lithos 106, 380–398.
Pang, K.-N., Chung, S.-L., Zarrinkoub, M.H., Khatib, M.M., Mohammadi, S.S., Lee, H.-Y., Chu, C.-H., Lin, I.-J., 2011. Eocene-Oligocene calc-alkaline magmatism in the Lut-Sistan region, eastern Iran: petrogenesis and tectonic implications. AGU Fall Meeting Abst. V43C-2598.
Pang, K.-N., Chung, S.-L., Zarrinkoub, M.H., Mohammadi, S.S., Yang, H.-M., Chu, C.-H., Lee, H.-Y., Lo, C.-H., 2012. Age, geochemical characteristics and petrogenesis of Late Cenozoic intraplate alkali basalts in the Lut-Sistan region, eastern Iran. Chemical Geology 306–307, 40–53.
Pang, K.-N., Chung, S.-L., Zarrinkoub, M.H. et al., in review. Iranian uptrapotassic rocks signify the initiation of post-collisional magmatism in the Arabia–Eurasia collision zone at 11 Ma. Terra Nova.
Pearce, J., Bender, J., De Long, S., Kidd, W., Low, P., Guner, Y., Saroglu, F., Yilmaz, Y., Moorbath, S., Mitchell, J., 1990. Genesis of collision volcanism in Eastern Anatolia, Turkey. Journal of Volcanology and Geothermal Research 44, 189–229.
Rahmati-Ilkhchi, M., Faryad, S.W., Holub, F.V., Kosler, J., Frank, W., 2011. Magmatic and metamorphic evolution of the Shotur Kuh metamorphic complex (Central Iran). International Journal of Earth Sciences 100, 45–62.
Ramezani, J., Tucker, R.D., 2003. The Saghand region, Central Iran: U–Pb geochronology, petrogenesis and implications for Gondwana tectonics. American Journal of Science 303, 622–665.
Rossetti, F., Nasrabady, M., Vignaroli, G., Theye, T., Gerdes, A., Razavi, M.H., Vaziri, H.M., 2010. Early Cretaceous migmatitic mafic granulites from the Sabzevar range (NE Iran): implications for the closure of the Mesozoic peri-Tethyan oceans in central Iran. Terra Nova 22, 26–34.
Saadat, S., Stern, C.R., 2011. Petrochemistry and genesis of olivine basalts from small monogenetic parasitic cones of Bazman stratovolcano, Makran arc, southeastern Iran. Lithos 125, 607–619.
Şengör, A.M.C., Kidd, W.S.F., 1978. Post-collisional tectonics of the Turkish–Iranian Plateau and a comparison with Tibet. Tectonophysics 55, 361–376.
Shabanian, E., Bellier, O., Siame, L., Arnaud, N., Abbassi, M.R., Cocheme, J.-J., 2009. New tectonic configuration in NE Iran: active strike-slip faulting between the Kopeh Dagh and Binalud mountains. Tectonics 28, TC5002 http://dx.doi.org/10.1029/2008TC002444.
Shafiei, B., Haschke, M., Shahabpour, J., 2009. Recycling of orogenic arc crust triggers porphyry Cu mineralization in Kerman Cenozoic arc rocks, southeastern Iran. Mineralium Deposita 44, 265–283.
Shahabpour, J., 2007. Island-arc affinity of the Central Iranian Volcanic Belt. Journal of Asian Earth Sciences 30, 652–665.
Shahbazi, H., Siebel, W., Pourmoafee, M., Ghorbani, M., Sepahi, A.A., Shang, C.K., Abedini, M.V., 2010. Geochemistry and U–Pb zircon geochronology of the Alvand plutonic complex in Sanandaj–Sirjan Zone (Iran): new evidence for Jurassic magmatism. Journal of Asian Earth Sciences 39, 668–683.
Sheibi, M., Esmaeily, D., Nedelec, A., Bouchez, J.L., Kananian, A., 2010. Geochemistry and petrology of garnet-bearing S-type Shir–Kuh Granite, southwest Yazd, Central Iran. Island Arc 19, 292–312.
Sláma, J., Košler, J., Condon, D.J., Crowley, J.L., Gerdes, A., Hanchar, J.M., Horstwood, M.S.A., Morris, G.A., Nasdala, L., Norbeg, N., Schaltegger, U., Schoene, B., Tubrett, M.N., Whitehouse, M.J., 2008. Plešovice zircon — a new natural reference material for U–Pb and Hf isotopic microanalysis. Chemical Geology 249, 1–35.
Stöcklin, J., 1968. Structural history and tectonics of Iran: a review. American Association of Petroleum Geologists Bulletin 52, 1229–1258.
Tatsumi, Y., Eggins, S., 1995. Subduction Zone Magmatism. Blackwell Science (211 pp.).
Valizadeh, M.V., Cantagrel, J.M., 1975. Premières données radiométiques (K–Ar et Rb–Sr) sur les micas du complexe magmatique du Mont Alvand, près Hamadan (Iran occidental). Comptes Rendus Académie des Sciences 281, 1083–1086.
Verdel, C., Wernicke, B.P., Ramezani, J., Hassanzadeh, J., Renne, P.R., Spell, T.L., 2007. Geology and thermochronology of Tertiary Cordilleran-style metamorphic core complexes in the Saghand region of central Iran. Geological Society of America Bulletin 119, 961–977.
Verdel, C., Wernicke, B.P., Hassanzadeh, J., Guest, B., 2011. A Paleogene extensional arc flare-up in Iran. Tectonics 30, TC3008 http://dx.doi.org/10.1029/2010TC002809.
Vernant, Ph., Nilforoushan, F., Hatzfeld, D., Abbassi, M.R., Vigny, C., Masson, F., Nankali, H., Martinod, J., Ashtiani, A., Bayer, R., Tavakoli, F., Chéry, J., 2004. Present-day crustal deformation and plate kinematics in the Middle East constrained by GPS measurements in Iran and northern Oman. Geophysical Journal International 157, 381–398.
Vincent, S.J., Allen, M.B., Ismail-Zadeh, A.D., Flecker, R., Foland, K.A., Simmons, M.D., 2005. Insights from the Talysh of Azerbaijan into the Paleogene evolution of the South Caspian region. Geological Society of America Bulletin 117, 1513–1533.
Walker, R., Jackson, J., 2004. Active tectonics and late Cenozoic strain distribution in central and eastern Iran. Tectonics 23, TC5010 http://dx.doi.org/10.1029/2003TC001529.
Walker, R.T., Gans, P., Allen, M.B., Jackson, J., Khatib, M., Marsh, N., Zarrinkoub, M., 2009. Late Cenozoic volcanism and rates of active faulting in eastern Iran. Geophysical Journal International 177, 783–805.
Wilmsen, M., Fürsich, F.T., Seyed-Emami, K., Majidifard, M.R., Taheri, J., 2009. The Cimmerian Orogeny in northern Iran: tectono-stratigraphic evidence from the foreland. Terra Nova 21, 211–218.
Zarrinkoub, M.H., Chung, S.-L., Chiu, H.-Y., Mohammadi, S.S., Khatib, M.M., Lin, I.-J., 2010. Zircon U–Pb age and geochemical constraints from the northern Sistan suture zone on the Neotethyan magmatic and tectonic evolution in eastern Iran. In: Dilet, Y., et al. (Ed.), Tectonic Crossroads: Evolving Orogens of Eurasia–Africa–Arabia, Ankara, Turkey: Geol. Soc. Amer. Abstract Volume, p. 54.
Zarrinkoub, M.H., Pang, K.-N., Chung, S.-L., Khatib, M.M., Mohammadi, S.S., Chiu, H.-Y., Lee, H.-Y., 2012. Zircon U–Pb ages and geochemical constraints on the origin of the Birjand ophiolite, eastern Iran. Lithos 154, 392–405.